5-2018

Yeast Two Hybrid Screen of a Putative Toxoplasma gondii Cyclin, TGME49_266900

Anna L. Schorr
Saint Cloud State University, alschorr@stcloudstate.edu

Yeast Two Hybrid Screen of a Putative *Toxoplasma gondii* Cyclin, TGME49_266900

by

Anna Schorr

A Thesis

Submitted to the Graduate Faculty of

St. Cloud State University

in Partial Fulfillment of the Requirements

for the Degree

Master of Science

in Cell and Molecular Biology

May, 2018

Thesis Committee:
Christopher Kvaal, Chairperson
Timothy Schuh
Nathan Bruender

Abstract

In this current research, protein-protein interactions with a putative *Toxoplasma gondii* cyclin, TGME49_266900 or "Cyc6," were discovered via a yeast two hybrid screen. Several putative interacting protein partners were isolated and described from a cDNA library of an asynchronous tachyzoite transcriptome. After false positives were weaned from the study, two proteins were identified as Cyc6 interacting partners. These two proteins are described from the toxodb.org bioinformatic database as a DJ-1 family protein (TGME49_214290) and a ThiF protein (TGME49_314890). Interestingly, the interacting DJ-1 protein has been shown in previous research to play a role in *T. gondii* microneme secretion. Additionally, ThiF proteins share distinct traits with E1 enzymes at the start of the ubiquitin pathway in eukaryotes. After no evidence of an interacting CDK partner for Cyc6 was obtained, a direct experiment was conducted testing for an interaction between Cyc6 and a putative CDK with expression levels notably higher in bradyzoites instead of tachyzoites. The outcome of this experiment showed no interaction between Cyc6 and the putative CDK. Although no interacting CDK partner was evident from this yeast two hybrid screen, two proteins were found to display a strong and biologically relevant interaction with the putative cyclin of interest. Future studies regarding Cyc6 should explore potential noncanonical roles for this putative cyclin in not only tachyzoites, but also bradyzoites and the purpose of Cyc6's interaction with the two proteins discovered from this screen.

Acknowledgements

It took two years and relentless support (in many forms) in order to achieve not only the following research, but also to foster my identity as a scientist and scholar. I began my Master's Degree at Saint Cloud State University with trepidation and an overwhelming sense of aimlessness. However, what had I lacked in practical skills and knowledge, I made up for in curiosity. My journey from a consumer to producer of knowledge was made possible by my advisor, Dr. Christopher Kvaal. Through the past two years, Dr. Kvaal did not give up or give in through the various obstacles I encountered in my research. My additional committee members, Dr. Timothy Schuh and Dr. Nathan Bruender knew my potential and did not let me take the easy route around difficult questions. The research I was fortunate to become involved in was made possible by Dr. Michael White and researchers from the University of South Florida as they provided key materials and also sequenced DNA without cost.

Attending Saint Cloud State University gave me a strong support system and foundation to continue on in my education beginning May 2018 in a doctoral program in Molecular & Cell Biology at Arizona State University. Credit needs to be given to Dr. Mary Rumpho-Kennedy and Dr. Kristin Gulrud who both supported me throughout this program and encouraged my continuous growth academically.

Finally, I would like to thank my parents who made a special trip from Mesa, AZ to attend my public thesis defense. The 25 years of unconditional support they've given me made this achievement (and many more in the past and future) possible.

Table of Contents

List of Tables

Table Page

List of Figures

Figure Page

List of Abbreviations

AD	Activating Domain
ATP	Adenosine Triphosphate
BD	Binding Domain
BLAST	Basic Local Alignment Search Tool
CDK	Cyclin Dependent Kinase
Cyc	Cyclin
Cyc6	*T. gondii* putative cyclin, TGME49_266900
DDO	Double Dropout
DJ-1	Protein Deglycase DJ-1, TGME49_214290
DMSO	Dimethyl Sulfoxide
EDTA	Ethylenediaminetetraacetic Acid
GRA	Dense Granule Protein
I-TASSER	Iterative Threading Assembly Refinement
LiAC	Lithium Acetate
OD	Optical Density
ORF	Open Reading Frame
QDO	Quadruple Dropout
QDO X-a-gal	Quadruple Dropout with X-
PCR	Polymerase Chain Reaction
PEG	Polyethylene Glycol
PVM	Parasitophorous Vacuole Membrane
RPM	Rotations per Minute
SDS	Sodium Dodecyl Sulfate
SOC	Super Optimal Broth
TBE	Tris Boric Acid EDTA
Tg	*Toxoplasma gondii*
ThiF	Thiamin Pyrophosphate Biosynthesis Protein F
YPD(A)	Yeast Extract Peptone Dextrose (Adenine)

Chapter I: Introduction

Apicomplexa

Within recent years, the life stages and cell cycle of apicomplexans have been the focus of several research efforts. While apicomplexans share many conserved pathways and proteins with other eukaryotes, many novel apicomplexan proteins distinguish these parasites from other phyla. The apicomplexan phylum consists of more than 5,000 species, many of which are obligate parasites that cause toxoplasmosis, malaria and cryptosporidiosis (Lorenzi et al., 2016; Francia & Striepen, 2014). Apicomplexans form a diverse phylum of obligate parasites which contain an iconic apicomplast to allow penetration into a host's cells. Other well known members in this phylum include the *plasmodium* and *cryptosporidium* genera. One particular parasite, *Toxoplasma gondii*, has received attention worldwide within the past few years with the infamous case of Martin Shkreli and Turing Pharmaceuticals.

Toxoplasma gondii

Similar to other apicomplexans, *T gondii* has an apicomplast (McFadden & Yeh, 2017) and other specialized organelles called micronemes to assist in host cell invasion (Sidik et al., 2016). Most apicomplexan parasites are limited to a small range of hosts such as insects and mollusks, yet *T. gondii* by comparison, has adapted to invading a diverse range of hosts including all warm blooded animals and birds (Lorenzi et al., 2016). *T. gondii's* success as an intracellular parasite can be attributed to its remarkable ability to thrive in an abundance of hosts and habitats.

Within *T. gondii*, three major clonal lineages, I, II and III are prevalent in humans and domestic animals (Paredes-Santos et al., 2015). Each lineage has distinct features, but a few features of importance are the virulence and capacity to form tissue cysts. The type I strain is

reported to have the highest rates of virulence in mice as indicated by amount of tachyzoites and rates of replication (Dardé, 2008). In comparison to the other strains, type I parasites have an enhanced ability to migrate throughout the host which is an explanation for why type I strains are more commonly seen migrating greater distances and through barriers such as the placenta in infected hosts (Saeij et al., 2005). In many scenarios, it is beneficial for the parasite to remain incognito as dormant tissue cysts in the host, although rapid replication may serve to be beneficial in some cases. Type II is most common in humans in western countries and is characterized by a lower virulence and greater ability to form dormant tissue cysts (Sullivan & Jeffers, 2001). In France, one of the countries with the highest rates of documented human toxoplasmosis, the type II strain reportedly compromises more than 90% of human toxoplasmosis cases (Ajzenberg et al., 2002). Type III strains also tend to be less virulent and form tissue cysts in comparison to type I but several samples from patients in South America and parts of Africa indicate parasites with a mixed genotype of type I and type III (Dardé, 2008; Sibley et al., 2009). Understanding the traits and transmission of the different strains of *T. gondii* help to track the pathogenesis of toxoplasmosis.

Toxoplasmosis

Toxoplasma gondii, the causative agent of toxoplasmosis, has serious consequences on the immunocompromised and fetuses. Conditions associated with toxoplasmosis include still births or instantaneous abortions, retinochoroiditis and toxoplasmic encephalitis. Although 30-50% of the world's population is estimated to be infected with *T. gondii*, it typically is thought of as asymptomatic in immunocompetent individuals (Flegr et al., 2014). While physical symptoms may be nonexistent in the majority of individuals with toxoplasma tissue cysts,

infrequent but deadly outbreaks of toxoplasmosis have occurred in immunocompetent populations (Demar et al., 2007). Additionally, recent findings suggest correlations between *T. gondii* and mental illnesses such as schizophrenia (Esshili et al., 2016). While it is acknowledged that causation cannot be derived from correlation, there is an agreement within the scientific community that *T. gondii* requires additional research regarding its several enigmatic functions within itself and upon hosts.

Congenital toxoplasmosis. *Toxoplasma gondii* was first discovered in 1908 and gained medical importance in 1939 due to the first reported case of congenital toxoplasmosis (Dubey, 2008). Toxoplasmosis represents a hazard to fetuses in utero if the mother becomes infected during pregnancy. Congenital toxoplasmosis refers to the condition when maternal transmission of toxoplasmosis to an unborn fetus occurs. Although most women residing in regions of a large toxoplasmosis seroprevalence have already been infected before pregnancy (Torgerson & Mastrolacovo, 2013) which equates to a strong maternal immunity (Sibley et al., 2009), the potential consequences on the fetus if the mother is infected mid pregnancy may be severe. More serious and pronounced congenital toxoplasmosis symptoms tend to manifest when the mother is infected in the earlier stages of pregnancy. Congenital toxoplasmosis is commonly associated with retinochroiditis, intracranial calcification and encephalitis (McAuley, 2014) besides fetal death.

Retinochoroiditis. *Toxoplasma gondii* is also responsible for up to 50% of the potentially blinding condition of retinochoroidits worldwide (Wallace & Stanford, 2008). Inflammation in the eye occurs when *T. gondii* tissue cysts rupture in the retina (Sibley et al., 2009) which will usually subside with vision restored in immunocompetent patients but may cause blindness with

recurring tissue cyst ruptures in immunocompromised patients (Wallace & Stanford, 2008). Interestingly, high rates of ocular diseases such as retinochoroiditis have been observed in immunocompetent adults living in regions such as Brazil, where recombinations of the type I genotype are frequent (Dardé, 2008).

Schizophrenia. Several studies indicate the correlation between cat ownership and schizophrenia (Fuller-Torrey et al., 2015). Since felines are the definitive hosts of *T. gondii*, it is hypothesized that oocysts shed by domestic cats in litter boxes are a method of infection in cat owners. Although additional longitudinal studies are needed to definitively conclude the causation of some cases of schizophrenia with *T. gondii* infection, many preliminary studies indicate a fair possibility of these two diseases having commonalities.

Immune Responses

Toxoplasma gondii and the human immune system play a delicate game of checks and balances. If *T. gondii* tachyzoites begin to grow too rapidly, the immune system will respond promptly. Due to the necessary components of both innate and adaptive immune systems, the immunocompromised are at a clear disadvantage in combating this opportunistic parasite.

Initially, the innate immune system will recognize key parasitic traits with Toll Like Receptors (TLRs) (Dupont et al., 2012) which are located in several cell types such as leukocytes, lymphocytes, endothelial and epithelial cells. Upon activation of the TLRs from the invading parasite, production of the cytokine interleukin-12 from dendritic cells stimulates natural killer (NK) cells and also T lymphocytes to produce interferon gamma (IFNγ) (Mashayekhi et al., 2011). IFNγ stimulates macrophages to eliminate *T. gondii* parasites and also induces production of nitric oxide which helps to halt *T. gondii* replication. Additionally, IFNγ

also promotes tryptophan degradation in infected cells which is seemingly beneficial as *T. gondii* is a tryptophan auxotroph (Dupont et al., 2012).

The adaptive immune system is crucial for specific targeting of cells harboring *T. gondii*. Dendritic cells, when presenting *T. gondii* antigens, will activate the appropriate helper and cytotoxic T cells for a specific and effective immune response. Cytotoxic CD8 T cells bind to and directly kill cells infected with *T. gondii* by secreting perforins and granzymes which activate caspase pathways (Krishnamurthy et al., 2017). CD4 T helper cells are crucial in the eradication and continued resistance to *T. gondii* infection. For example, CD4 T cells provide crucial signals to activate CD8 T cells and B cells which produce antibodies to provide humoral immunity (Dupont et al., 2012). Without functional CD4 or CD8 T cells, *T. gondii* parasites have no consistent pressure to prevent uncontrolled replication (Wallace & Stanford, 2008). Therefore, it is apparent immunocompromised individuals, such as HIV/AIDS patients with a depleted CD4 T cell repertoire, will struggle to stifle *T. gondii* infections.

While all of these processes occur during the rapidly proliferating like stage of *T. gondii,* the formation of a slow growing nonimmunogenic tissue cyst helps to protect the parasite from detection from the immune system. Conversion from the slow growing bradyzoite tissue stage to the rapidly proliferating tachyzoite stage may occur without proper mediation from the immune system (Eaton et al., 2006).

Current Treatments

Typically toxoplasmosis does not require intervention with antibiotics in immunocompetent hosts, but the immunocompromised and pregnant women rely on specific medications to combat the parasite. Medications such as a combination of pyrimethane and

sulfadiazine are used to combat acute toxoplasmosis, or the rapidly proliferating tachyzoite stage. Unfortunately, no medication is currently used to target the dormant bradyzoite stage (Sullivan & Jeffers, 2011) even though this stage can rapidly differentiate back into the tachyzoite stage as evidenced in HIV/AIDS patients and in mice (Skariah et al., 2010).

Transmission

Toxoplasma gondii relies on warm blooded animals and birds as intermediate hosts to eventually make its way to its definitive host, felines. Several methods of transmission exist between felines, humans and other warm blooded hosts but all involve the ingestion of the parasite in some form or the parasite crossing into the placenta. The parasite must travel through the acidic gastric juices of all new hosts, which is commonly done in the bradyzoite life stage in which the parasite is in a protective capsule, called a parasitophorous vacuole (Skariah et al., 2010). As the cysts travel through the stomach, the vacuole walls resist digestion in HCl but are destroyed in the presence of pepsin or trypsin (Dubey & Jones, 2008). Once inside the intestines, bradyzoites or sporozoites (if from sexual reproduction) will invade the host's intestinal epithelium and quickly differentiate into tachyzoites (Skariah et al., 2010).

To people. Humans are infected by *T. gondii* by several possible routes. Consuming undercooked meat of infected animals is a common cause of infection, especially in cultures where undercooked meat is commonly consumed, especially France (Hill & Dubey, 2002). Other possible routes of infection include ingestion of oocysts found in feline feces by cleaning litter boxes or consuming crops contaminated with fecal oocysts. In central and South America, high rates of toxoplasmosis have been attributed to environmental contamination and ingestion of oocysts, which is considered to be another common form of transmission (Dubey & Jones,

2008). When considering livestock operations, it is well known cats and farmers share a sort of mutualistic relationship. Cats live in barns for shelter from the elements, or perhaps other predators and return will hunt rodents which are considered to be a nuisance. Since felines are the definitive hosts for *T. gondii*, the abundance and proximity of oocysts in feline feces causes livestock to be at a greater risk to be infected with *T. gondii* (Dubey & Jones, 2008). As previously discussed, congenital toxoplasmosis is transmitted from pregnant women to fetuses, which was the first case of toxoplasmosis observed in humans in 1939 (Weiss & Dubey, 2009). In rare cases, toxoplasmosis has been transmitted through organ transplants of infected organs (Dubey & Jones, 2008). *Toxoplasma gondii'*s strategies in developing hardy oocysts that can maintain viability in the environment without a host and the robust cyst walls that resist degradation in stomach acid prove to be formidable tactics in host invasion.

To cats. Although *T. gondii* may cause havoc in humans, the ultimate goal of this parasite is to sexually reproduce within a feline host. *Toxoplasma gondii* has demonstrated the ability to manipulate the behavior of rodents to make them more accessible to be eaten by a feline predator. Such behavior changes in rodents include an increase in exploratory behavior and inhibition of fear of felines (Stock et al., 2017). Although the rodent host is more likely to be killed, the tissues containing *T. gondii* cysts are released in the intestines of the feline host which allows for parasitic sexual reproduction. Examination of brains of rodents infected with *T. gondii* indicate a noticeable accumulation of tissue cysts around the amygdala, which functions in fear responses (Vyas et al., 2007). Therefore, it is theorized rodents are inhibited towards sensing fear in the presence of one of their main predators, felines, which makes them easy targets for *T. gondii*'s definitive host.

Life stages

Toxoplasma gondii has distinct life stages which allow the parasite to invade cells of hosts, evade host immune systems and to reproduce sexually and asexually (Figure 1). Life stages related to sexual reproduction, sporozoites and oocysts are present only in felines or directly shed from felines into the environment. Contaminating oocysts shed through feces or bradyzoites consumed through an infected intermediate host have a durable outer shield to protect the parasite until it is ingested by a new host. After an intermediate host is infected, signals are given to the cyst to enter the rapidly replicating tachyzoite stage. Due to its ability to form dormant tissue cysts, *T. gondii* may persist for the entirety of the host's life (Pappas et al., 2009). While *T. gondii* will usually exist in the bradyzoite stage in immunocompetent hosts, it has shown the ability to transition back into the tachyzoite stage in the same host (Huang et al., 2017). Several studies indicate parasite replication is crucial for virulence and is an underlying factor for disease severity with apicomplexan parasitic infections (Gubbels et al., 2008). The ability for *T. gondii* parasites to oscillate between various life stages in to persist within hosts is a crucially important yet enigmatic area of research.

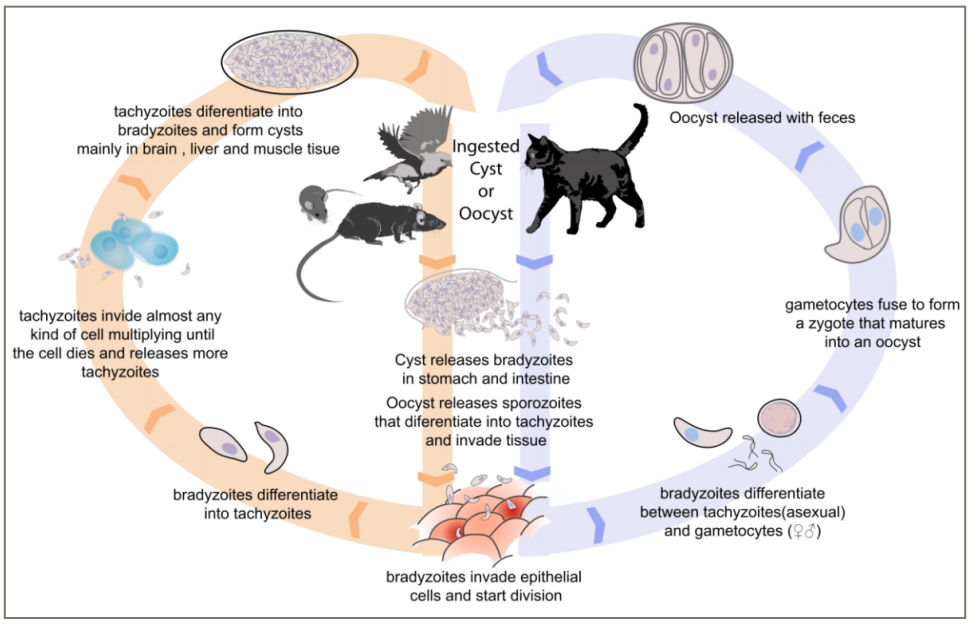

Figure 1: The Life Cycle of *T. gondii.* This apicomplexan's life cycle includes both sexual and asexual reproduction. Warm blooded animals or birds are the intermediate hosts for these parasites (image courtesy of Wikipedia Commons).

Sporozoites & Oocysts. After sexual reproduction and passage through feces in feline hosts, the stable oocyst, which contains sporozoites, may persist for months in the environment until it is able to infect a new host (Pappas et al., 2009). Infected felines may shed up to 55 million oocysts per day for approximately eight days (Torrey & Yolken, 2013). Despite the multitude of oocysts and sporozoites produced within the feline host, there are rarely clinical signs of *T. gondii* infection in felines compared to intermediate hosts such as rodents and humans (Dubey, 1998).

Tachyzoites. After infecting an intermediate host, *T. gondii* enters the tachyzoite life stage, which is characterized by rapid cell replication. When an intermediate host becomes infected by consumption of oocysts or tissue cysts containing bradyzoites, the intestinal epithelium is invaded and differentiation to the tachyzoite stage occurs (Skariah et al., 2010).

Then rapid replication occurs by endodyogeny with two daughter cells forming within one mother cell (Sullivan & Jeffers, 2011). In immunocompetent hosts, an IFNγ dependent cell mediated immune response eradicates most of the parasite after infection. However, a few tachyzoites can escape the host's immune system by localizing to areas of the central nervous system and muscle tissue (Skariah et al., 2010). Due to rapid proliferation, *T. gondii* tachyzoites have been used as model organisms to study the novel cell cycle in apicomplexans (Eaton et al., 2006). Tachyzoites persist in this life stage in humans for approximately 10-14 days after infection before they differentiate into the bradyzoite life stage (Lyons et al., 2002).

Bradyzoites. After rapid replication and relocating to specific host tissues, tachyzoites will typically differentiate into the dormant, or slow growing bradyzoite stage. This differentiation is characterized by slowed replication and metabolism, and expression of bradyzoite-specific proteins (Eaton et al., 2005) which direct the parasite to form dormant tissue cysts among other traits. Tissue cysts may be as small as 5 μm in diameter and only contain two bradyzoites or cysts may be as large as 70 μm in diameter and contain up to 1,000 bradyzoites (Dubey et al., 1998). Due to the formation of tissue cysts, slowed growth, and lack of immunogenicity, bradyzoites are able to evade detection from the host's immune system to ensure long term viability in tissue (Kim, 2015). Bradyzoite tissue cysts are typically found in parts of the central nervous system, skeletal and cardiac muscles and the eyes but have also been found in organs including lungs, liver, kidneys and bone marrow (Skariah et al., 2010). While the tissue cysts are not immunogenic, periodic ruptures of these cysts releasing bradyzoites is thought to contribute to maintaining immunological memory against *T. gondii* in infected hosts (Filisetti & Candolfi, 2004).

Interconversion between Tachyzoites and Bradyzoites. Pressure from the immune system and stress inducing environments promotes tachyzoite to bradyzoite differentiation. Tachyzoite to bradyzoite conversion is observed in the presence of nitric oxide, which is produced by inducible nitric oxide synthase (iNOS). One function of IFNγ is to stimulate macrophages to produce iNOS with which the production of nitric oxide asserts pressure on the parasite to slow replication and convert to the dormant bradyzoite stage (Dupont et al., 2012). A popular technique in lab studies involving bradyzoites is to expose cells infected with *T. gondii* tachyzoites to alkaline conditions to initiate the up regulation of bradyzoite specific proteins (Huang et al., 2017). Bradyzoite conversion is also achieved with heat shock, which may be caused by fevers within intermediate hosts (Lyons et al., 2002). However, *T. gondii* has been shown to transition back into tachyzoites from the bradyzoite life stage under appropriate conditions which can allow the parasite to invade new tissues only to transition back into bradyzoites. In the absence of IL-12, CD4 or CD8 T cells and IFNγ, bradyzoites have been observed to convert back into the tachyzoite life stage (Lyons et al., 2002; Dupont et al., 2012). This interconversion may be fatal to immunocompromised individuals, even those who had dormant tissue cysts for years before developing an immunodeficiency (Skariah et al., 2010). Recent research has focused on the pathways and factors governing the interconversion between these two life stages.

Cell Cycle

One possible avenue to combat *T. gondii* infections is to investigate the cell cycle and determine possible strategies to disrupt or halt cell growth. Since host death is possibly due to the repeated cycles of parasitic replication, host cell invasion and host cell lysis, disrupting *T.*

*gondii'*s cell cycle theoretically would prevent adverse symptoms or death in susceptible populations. *T. gondii* has a distinct cell cycle, that differs from most eukaryotes, which have four distinct cell cycle phases. Additionally similar to other novel apicomplexan cell division schemes, *T. gondii* replicates asexually by endodyogeny in addition to sexual reproduction. Although there are several differences between apicomplexan and other Eukaryotic cell cycles, a few core traits persist throughout the entire domain. Such traits include mitosis, dividing chromosome replicates into daughter cells, and regulatory cyclin and cyclin dependent kinases (Francia & Striepen, 2014). For example, three cyclin dependent kinase subfamilies, which have roles in the cell cycle, are only found in apicomplexans and not in other Eukaryotes (Talevich et al., 2011). Therefore, we cannot rely solely on bioinformatic queries to investigate and draw conclusions on the mechanisms and proteins involved in apicomplexan cell cycles.

***Toxoplasma gondii* Cell Cycle.** Not only do apicomplexan cell cycles differ from other Eukaryotes in a few distinct ways, but within *T. gondii* itself, there are differences in cell cycles between life stages. The general pattern of Eukaryotic cell cycle phases in order are Gap 1 (G1), Synthesis (S), Gap 2 (G2), Mitosis (M) and Cytokinesis (C). A major difference between the typical Eukaryotic cell cycle and apicomplexa is that G2 phase of the cell cycle is seemingly absent in most apicomplexans (Alvarez & Suvorova, 2017) as seen in Figure 2. Interestingly, the G2 phase has been identified in *T. gondii* parasites transitioning from tachyzoites to bradyzoites (Gubbels et al., 2008).

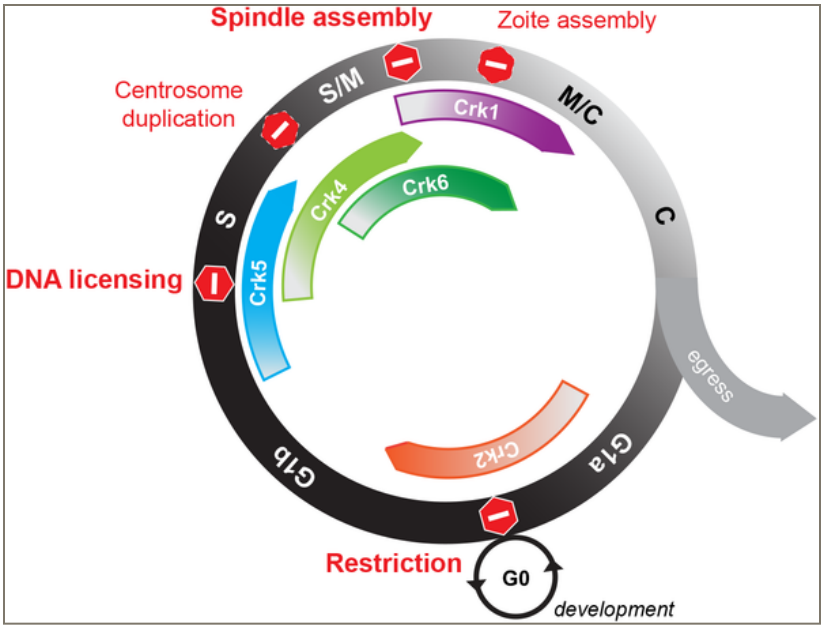

Figure 2: *Toxoplasma gondii* Cell Cycle. The *T. gondii* cell cycle with specific cyclin related kinases each phase is shown above (Alvarez & Suvorova, 2017).

Specific features are used to mark the progression of *T. gondii* through the cell cycle which research has predominantly based on tachyzoite protein expression and morphologies due to bradyzoite cell cycle arrest in G0 or G1 phases (Gubbels et al., 2008). Since bradyzoites are halted at either of these stages they rarely progress, if at all through the cell cycle which necessitates studying the cell cycle via tachyzoites. The G1 phase of the *T. gondii* cell cycle accounts for nearly half of the total time tachyzoites spend in the active cell cycle (Alvarez & Suvorova, 2017). The G1 phase is characterized by preparation for chromosome replication and lastly centrosome replication which leads directly into the S phase (Francia & Striepan, 2014; Gubbels et al., 2008). Chromosome replication is the main event of S phase along with centrosome migration to the apical side of the nucleus (Gubbels et al., 2008). The G2 phase is mostly or completely bypassed as the cell moves into M phase. During mitosis, chromosome replication is completed and a set of chromosomes for the new daughter cells are pulled towards

spindle poles in separate areas in the apical side of the nucleus. Throughout cytokinesis, proteins involved in the inner membrane complex and formation of the daughter cell cytoskeletons are expressed (Gubbels et al., 2008). The final steps in cytokinesis mark the end of the cell cycle as the two newly formed daughter cells resolve from the mother cell and become two independent cells (Behnke et al., 2010). Throughout each phase, a set of cyclins and cyclin dependent kinases act as regulators determining the progression through the cell cycle (Kvaal et al., 2002).

Cyclins and Cyclin Dependent Kinases

Cyclins and cyclin dependent kinases (CDKs) are two large, conserved families of proteins which regulate the cell cycle of Eukaryotes. Even though these protein families are conserved, there are several novel cyclins and CDKs in the apicomplexan phylum (Peixoto et al., 2010). The term "cyclin" was coined due to the fluctuation, or cycling, of these proteins' expressions throughout the different stages of the cell cycle. Cyclin expression increases by regulation from specific transcription factors and their expression wanes with ubiquitin-directed destruction (Francia & Striepen, 2014). When a cyclin interacts with a corresponding CDK, the CDK structure reconfigures to reveal a molecule of ATP with which it is able to phosphorylate a target substrate. Phosphorylation by active CDKs may induce a multitude of pathways, many of which allow the cell to progress through the cell cycle (Morgan, 2007), but cyclin and CDK complexes are also known to have the ability to regulate transcription, RNA processing, translation and development (Alvarez & Suvorova, 2017).

Due to the importance of cyclin and CDK interactions in regulating cell cycle progression, an area of research that has the potential to provide solutions to parasitic infections and consequential illnesses is the identification and mapping of these specific protein-protein

interactions. However *T. gondii* does not have a fully annotated genome and many transcribed DNA sequences are labeled as "putative" or "hypothetical" proteins. Therefore, investigating protein interactions with proteins hypothesized to have a role in the cell cycle may provide clarity to the various enigmatic functions of *T. gondii* replication and allow additional annotation of the *T. gondii* genome.

TGME49_266900 . Due to the important role cyclins and cyclin dependent kinases play in regulating the cell cycle, proteins that appear to have these functions are prioritized in several studies. While many novel proteins exist in the apicomplexa phylum and in *T. gondii*, bioinformatic search engines provide starting points in protein-protein interaction experiments to hypothesize about a protein's function and interacting partners. The protein chosen to screen in this current study has features that are characteristic of a specific type of cyclin and are identified by bioinformatic databases such as toxodb.org and NCBI. Due to overlapping acronyms throughout the Eukaryotic domain and confusion with similar proteins of other species, the most reliable way to refer to *T. gondii* proteins is by the toxoID which provides the strain of *T. gondii* and a specific number in each name for each gene in the genome. Although the protein focused on in this study, TGME49_266900, has yet to be confirmed a cyclin, for brevity's sake it will be referred to as "Cyc6," keeping consistency with previous but pertinent studies (Alvarez & Suvorova, 2017).

Several bioinformatic search engines and protein prediction software have indicated the amino acid sequence of Cyc6 shares a high degree of similarity to other N-terminus containing cyclins (toxodb.org, iTASSER). Cyclins are identifiable by a tertiary structure containing two domains of five alpha helices each (Figure 3). The first bundle of helices is typically about 100

amino acids long and is known as the cyclin box where CDK binding occurs (Morgan, 2007). Cyc6 has a discernible cyclin box region which spans the typical cyclin box length from amino acid position 96 to 194 (ToxoDB.org, *Toxoplasma gondii* ME49). Classifying Cyc6 as a cyclin is supported by the indication from bioinformatic software used in previous studies of a "D-box," or Death box motif which initiates protein degradation that contributes to the characteristic cycling expression pattern (Alvarez & Suvorova, 2017; Morgan, 2007). However the scope of identifying cyclins with bioinformatic searches relies mostly on these two traits (a conserved cyclin box and a destruction motif for ubiquitination) which are detected based on BLASTp query outputs. Beyond these two identifiable features, cyclins have great variability which generates classes of cyclins unique to different phyla. For example, canonical A, B, D or E types of cyclins, which are familiar to higher Eukaryotes, have not been identified in *T. gondii*. Instead, only cyclins that are related to P, H, L and Y types have been observed (Alvarez & Suvorova, 2017). One interesting similarity between apicomplexa and other Eukaryotes is the presence of the conserved Y-type cyclin.

Figure 3: I-TASSER Cyc6 Model. Shown above is the predicted model of Cyc6 from iTASSER bioinformatic software.

Cyclin Y. According to analysis of bioinformatic software conducted by Alvarez and Suvorova in 2017, Cyc6 has similarities to the conserved Y-type cyclin. Despite being highly conserved, little is known about this recently discovered cyclin category (Liu et al., 2010). Among metazoan phyla, the Y-type cyclin is the most highly conserved cyclin besides cyclin C (Liu & Finley, 2010). To further demonstrate the high degree of conservation, the Y-type cyclin box has been identified in non-metazoan kingdoms such as plants and fungi. In addition, the Y-type cyclin box is more closely conserved when comparing yeast and plant to human and Drosophila cyclin domains than any other type of cyclin (Liu et al., 2010).

The *T. gondii* protein Cyc6 has apparent similarities to other Y-type cyclins as indicated by BLASTp outputs. A key component needed to create a hypothesis regarding Cyc6 interactions is comparing Y-type cyclins and their protein interactions across phyla. When the amino acid

sequence of Cyc6 was queried in the I-TASSER server, bioinformatic software using multiple algorithms to generate models and function predictions of proteins, similarities between Cyc6 and other cyclins were evident.

From the top 10 closely matching templates generated by the iTASSER server, two closely related yeast cyclins, PHO80 and Pcl10 were identified as being structurally similar to Cyc6. Both of these yeast cyclins belong to the PHO80p subfamily of cyclins that interact with PHO85, a multifunctional CDK (Andrews & Measday, 1998). While PHO85 is considered a non-essential CDK, it is involved in major roles such as phosphate metabolism, glycogen biosynthesis, actin regulation and cell cycle progression (Moffat et al., 2000).

Other CDK partners for Y-type cyclins have been identified throughout Eukaryotes. For example, the human Y-type cyclin was discovered in a yeast two hybrid screen conducted by Jiang et al. (2009) attempting to find a cyclin partner for PFTK1 or now referred to as CDK14. Additionally CDK16, a human CDK abundantly found in the Purkinje and pyramidal cells in the hippocampus, was found to interact with this cyclin (Mikolcevic, Rainer & Geley, 2012) and is essential for spermatogenesis (Mikolcevic et al., 2012). The cyclin Y homolog in *Drosophila* was found to be essential for development and played a role in Wg (WNT protein) signaling (Mikolcevic, Rainer & Geley, 2012). Eventually the link between cyclin Y and WNT protein signaling was established in vertebrates. Activation of a WNT co-receptor, LRP6, is achieved by phosphorylation from PFTK1/CDK14 kinases, which are activated by Y type cyclins (Davidson & Niehrs, 2010). A conserved trait among many eukaryotic Cyclin Y:CDK complexes is localization to the plasma membrane. The distinct N-terminal myristoylation signal of Cyc Y allows for localization of Y-type cyclins to the plasma membrane, where interacting CDK

partners are recruited to (Liu et al., 2010). While it cannot be expected a Y type cyclin from *T. gondii* would participate in homologous pathways or roles found in other Eukaryotic kingdoms, there may be parallels in established Y type cyclin protein interactions and apicomplexans.

AP2IX-4. Hemagglutinin tagged Cyc6 has been shown to be present during the tachyzoite stage with a peak expression during the G1 phase, yet in mutants without a functional Cyc6 protein, it was apparent that Cyc6 was not necessary for tachyzoite replication (Alvarez & Suvorova, 2017). However, no Additionally, Cyc6 did not interact with seven tested CDKs, or putative CDKs, in the tachyzoite cell cycle (Alvarez & Suvorova, 2017). Interestingly, Cyc6 was previously shown to be up regulated when transcription factor, AP2IX-4 was present. AP2IX-4 is up regulated when tachyzoites differentiate into bradyzoites during periods of cellular stress (Huang et al., 2017). lf Cyc6 is a cyclin, it is seemingly paradoxical that it would be up regulated in the slow growth stage yet be present in the G1 phase in tachyzoite growth. Therefore Cyc6 may play an important role in the transition between life stages.

Yeast Two Hybrid System

The yeast two hybrid system is a well established lab technique and is a relatively simple and cost efficient method for screening a genome for protein interactions. As the name suggests, this technique relies on phenotypic changes in attenuated two yeast strains to detect interacting proteins. Two interacting proteins will allow the GAL4 transcription factor binding and activating domains to come into close proximity to initiate transcription of a reporter gene to select for only interacting proteins as shown in Figure 4.

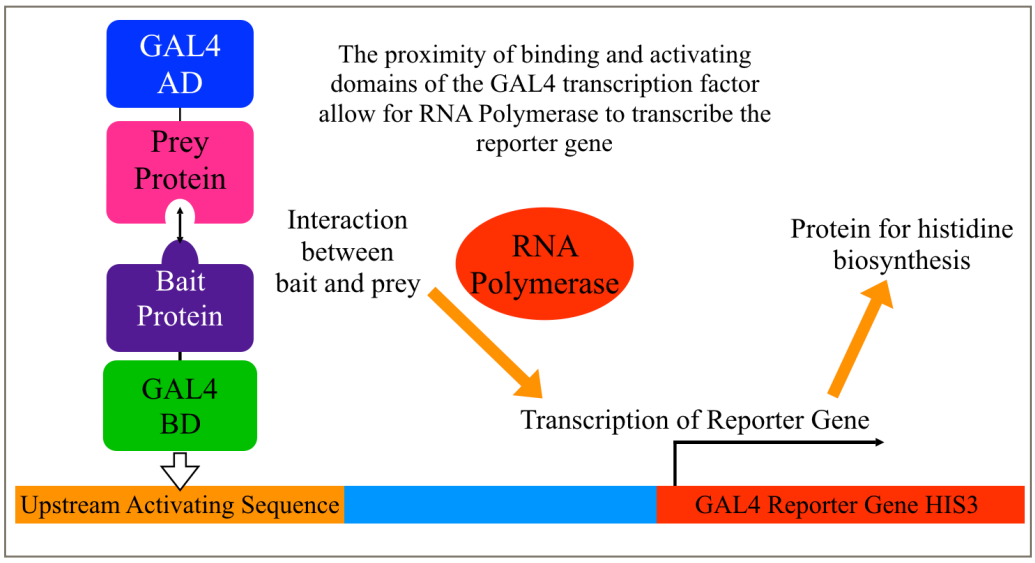

Figure 4: Schematic of the Yeast Two Hybrid System. The combination of both activating and binding domains of the GAL4 transcription factor allows for transcription of proteins in the biosynthetic pathway of histidine and adenine and for α-galactosidase, an enzyme which cleaves X-α-gal substrate to produce a blue hue.

Two attenuated strains of *Saccharomyces cerevisiae* are used to mate to produce diploids containing both the DNA insert of the protein of interest and a fragment of DNA from the cDNA library. Strains Y2HGold and Y187 are lacking functional genes for proteins in the biosynthetic pathways of tryptophan and leucine. By transformation with complimentary plasmids, the abilities to produce tryptophan and leucine are restored. Additionally, Y2HGold and Y187 are unable to produce histidine without a functional GAL4 transcription factor.

The yeast two hybrid system utilizes plasmids containing functional genes to complement the attenuated yeast strains as shown in Figure 5. Protein of interest inserts and cDNA library fragments are located in the multiple cloning sites of pGBKT7 and pGADT7 respectively. The protein of interest insert in pGBKT7 is cloned in frame with the binding domain of the GAL4 transcription factor. The cDNA library fragments in pGADT7 are in open reading frame with the

GAL4 activating domain. When two proteins interact, the binding and activating domains of GAL4 come into close proximity to create a functional transcription factor.

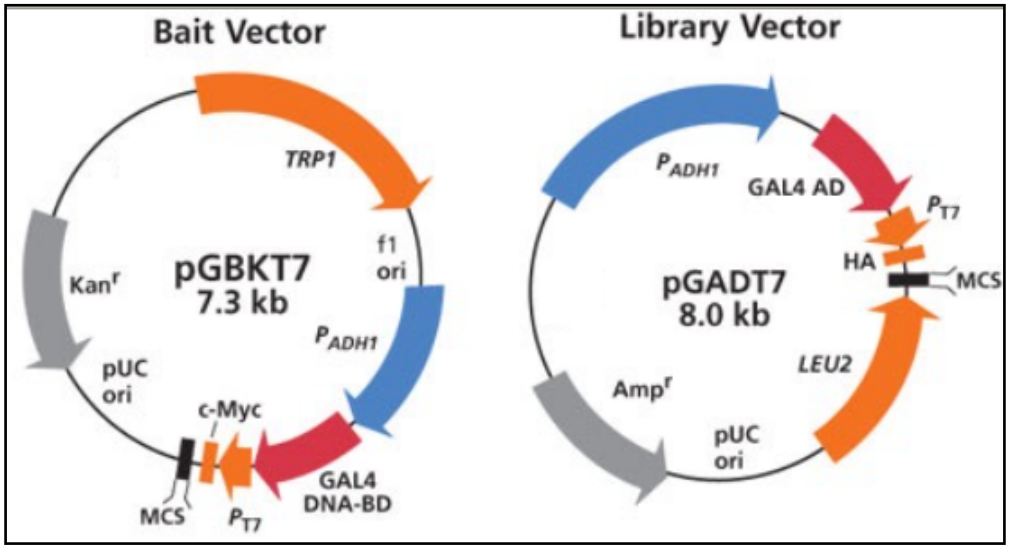

Figure 5: Yeast Two Hybrid Plasmids. The bait and library (prey) vectors contain sequences for selectable markers and for either the binding or activating domain of GAL4. The pGBKT7 vector contains sequences for kanamycin resistance, production of a functional protein in the biosynthetic pathway for tryptophan and the binding domain of GAL4. The pGADT7 vector contains sequences for ampicillin resistance, production of a functional protein in the biosynthetic pathway of leucine and the activating domain of GAL4.

Limitations

Bioinformatic technology has rapidly expanded in accuracy and availability within the past decade and the yeast two hybrid screen is a common and reliable lab technique. However, there are numerous limitations when relying on these strategies. Carefully planned methodology and experiments help to circumnavigate such pitfalls.

While the proteomes of many eukaryotes have been extensively studied and characterized, the apicomplexan phylum contains novel proteins that do not have homologies in any other eukaryotic phylum. Additionally, apicomplexans have a unique cell cycle which seems

to bypass the G2 phase (Gubbels et al., 2008). Due to this fundamental difference, novel apicomplexan cyclins without homologies in other eukaryotic phyla may provide misleading bioinformatic query results. While bioinformatic software may indicate key features in this proteins to characterize them into families, the user of such software must acknowledge that there is a possibility for error in computer derived predictions.

Several factors exist that may impact the results of yeast two hybrid screens and are of enough potential to disclose. There is substantial evidence that Cyc6 is up regulated in the bradyzoite stage of *T. gondii*. However the creation of the cDNA library in use was constructed from tachyzoites, not bradyzoites. Therefore any interactions between proteins up regulated during the bradyzoite stage or specific only to the bradyzoite stage may not be observed in this current yeast two hybrid screen. As Cyc6 is present during the tachyzoite stage but is down regulated after the G1 phase, it is expected to have at least one protein interaction involving its degradation expressed in the tachyzoite life stage which should be evident in this screen. A limitation of the yeast two hybrid system itself is that all of the interactions between Cyc6 and interacting protein partners must take place in the nucleus. If Cyc6 were to interact with a specific protein only in conditions outside of the parasitic nucleus, it may not be observed in the yeast two hybrid system. However it has been shown in the tachyzoite life stage that Cyc6 is localized to the nucleus (Alvarez & Suvorova, 2017) but it is uncertain if this information can be extrapolated to the bradyzoite life stage as well. Lastly, proteins often form interactions with more than one other protein at a time. For example, CDK inhibiting proteins bind to cyclin-CDK complexes (Morgan, 2007). Since only two *T. gondii* proteins are expressed in one diploid yeast cell at a time, such interactions may not be observed.

There are limitations with using a cDNA library that need to be acknowledged. Due to the process of producing a cDNA library with reverse transcriptase, there is a limit to the length of cDNA fragments made. The possibility of a number of nucleotides in a continuous transcribed gene being greater than the maximum length created by reverse transcriptase is almost certain. Therefore the DNA inserts of protein sequences in the cDNA library will not be of all genes in full length; the inserts will be of fragments of genes too large in nucleotide length to be transcribed by reverse transcriptase.

Extra experiments may be carried out in order to avoid some implications of these potential limitations. A major goal of this current research is to investigate whether or not this putative cyclin is truly a cyclin or if there could be an error from bioinformatic calculations. Protein interactions detected by the yeast two hybrid screen provide additional evidence for the purpose of this protein of interest. For example, if a cyclin dependent kinase partner is discovered through this screen, it would support the bioinformatic software's predictions. However, a cyclin dependent kinase partner may not be discovered either due to misidentification of Cyc6 being a cyclin or a cyclin dependent kinase partner may exist, but due to the limitations of the yeast two hybrid screen, it may not be identified due to a false negative error. A future research project with this protein of interest could include screening against a cDNA library derived from a life stage other than tachyzoite. Additionally, it is possible to order synthetic, full length DNA sequences of proteins to test with Cyc6 to avoid the problem of truncated sequences from the cDNA library. However, ordering synthetic DNA sequences is costly; sequences must be carefully selected with solid reasoning.

Chapter II: Hypotheses

As explained previously, bioinformatic software has suggested Cyc6 may be a Y-type cyclin. Cyc6 is up-regulated when transcription factor, AP2IX-4, is expressed. Intriguingly, Cyc6 is also not essential for tachyzoite growth but is seen to have a peak expression in the G1 phase of tachyzoites. By taking into account these unique traits associated with this putative cyclin, the following hypotheses have been derived:

1. Cyc6 interacts with proteins localized in the nucleus during the tachyzoite life stage
2. Cyc6 interacts with a kinase that has homology to CDKs in other organisms that also interact with a Y type cyclin, more specifically TGME49_285160

In order to maintain all hypotheses as falsifiable, it is necessary to exclude legitimate hypotheses pertaining to specific life stages that do not have accessible cDNA libraries. Therefore, hypothesis #2 specified a protein to directly test against Cyc6.

Chapter III: Materials and Methods

Bait Plasmid Construction

The Cyc6 sequence in prey plasmid, pGADT7, was provided by Dr. Michael White and researchers from the University of South Florida. Primers containing restriction enzyme sites for *NdeI* and *EcoRI* and the 5' and 3' ends of the Cyc6 insert were designed to amplify the insert in the open reading frame:

NdeI
Forward Primer: 5' *GAG CAT CAT ATG GCT GAG GAT AGC GTT CC* 3'

Reverse Primer: 5' *TTG AAT TCT CAG GAC ATT GTC TCG GC* 3'
EcoRI

The insert was amplified via PCR. Gel electrophoresis of the amplified sample with a 1.2% (w/v) gel was ran at 150V for one hour alongside an empty pGADT7 vector which confirmed successful amplification of the insert. The insert was extracted and purified from the agarose gel with a DNA Extraction Kit from IBI/MidSci.

To construct the bait plasmid, a 3:1 molar ratio of the pGBKT7 vector and amplified insert, respectively, were used. One hundred nanograms of the pGBKT7 vector and 60 ng of the amplified Cyc6 insert were digested with NEB *EcoRI HF* and *NdeI* restriction enzymes overnight at 37°C. The digested, linear vector and insert were ran in a 0.8% (w/v) agarose gel at 200V for 80 minutes alongside a 1kb ladder and then excised by a razor blade. The vector was dephosphorylated with NEB shrimp alkaline phosphatase and ligated with the Cyc6 insert with NEB T4 DNA ligase.

Successful subcloning of the Cyc6 insert into the pGBKT7 vector was indicated by 1.0% (w/v) agarose gel electrophoresis ran at 100V for 80 minutes following a double *EcoRI HF* and *NdeI* digest. Five hundred picograms of pGBKT7-Cyc6 plasmid were used to transform 100 µL of NEB *E. coli* strain DH5α competent cells. Successful transformations were selected by plating on LB agar containing ampicillin (50 µg/mL). The positive control with XPMC2 was supplied from NEB. The pGBKT7-Cyc6 plasmid was purified with an IBI mini-prep plasmid kit and then was assessed for purity and concentration at wavelengths of 260 nm and 280 nm with a Nanodrop 2000 spectrophotometer and software.

Bait Strain Transformation. Yeast strain Y2HG was transformed with the constructed bait plasmid. Cells from a glycerol stock of Y2HG were grown on YPDA agar for three days and three colonies (about 2-3 mm in diameter) were inoculated in 50 mL of liquid YPD and incubated at 30°C with shaking at 250 rpm overnight. From the overnight culture, 30 mL was added to 300 mL of fresh YPD and incubated at 30°C with shaking at 230 rpm. Cells were harvested after three hours by centrifugation at 1000x*g* for 5 minutes twice to consolidate the entire pellet. The resulting pellet was resuspended in 1.5 mL of 1x TE/LiAc. One hundred nanograms of pGBKT7-Cyc6 DNA was combined with 100 ng of Clontech carrier DNA to which 100 µL of the resuspended cell pellet was added and vortexed. Six hundred microliters of 1x PEG/LiAc solution was added to the suspension and vortexed on high speed for ten seconds. The cells were incubated at 30°C for 30 minutes with shaking at 200 rpm. After incubation, 70 µL of 100% DMSO was added and mixed by gentle inversion. The cells were heat shocked at 42°C for 15 minutes then chilled on ice for two minutes. The cells were harvested at 14000x*g* for

five seconds, then resuspended in 0.5 mL of sterile 1x TE buffer. To select for transformed cells, serial dilutions of 1:1 to 1:10000 were plated on tryptophan dropout media.

Yeast Two Hybrid Screen

For mating, a single three day old Y2HG pGBKT7-Cyc6 colony (approximately 3 mm in diameter) was selected and grown in 50 mL of tryptophan dropout media with added kanamycin (50 µg/mL) for 18 hours at 30°C while shaking at 250 rpm which gave an OD_{600nm} of 1.28. The cells were pelleted at 1000x*g* for 5 minutes. The pellet was resuspended in 5 mL of tryptophan dropout media and then the cells were counted in a hemocytometer to ensure proper density of the bait strain. One milliliter of a glycerol stock of *Saccharomyces cerevisiae* cell strain Y187 containing plasmids of the cDNA library in pGADT7, provided by the White lab of USF, were thawed at room temperature and 10 µL of the cDNA library were removed to prepare serial dilutions to plate on leucine dropout plates to check the prey strain viability. Forty five milliliters of 2x YPDA and kanamycin (50 µg/mL) were added to a sterile 2 L flask. Then 5 mL of the bait strain and 1 mL of the library strain were combined in the 2x YPDA. The vial containing the library strain was rinsed with 1 mL of 2x YPDA twice to ensure the maximum amount of cells were used in the mating. The 2 L flask was incubated at 30°C for 24 hours while shaking at 50 rpm. The mated cells were pelleted at 1000x*g* for 5 minutes. The flask was rinsed twice with 50 mL of 2x YPDA to ensure the maximum amount of mated cells were collected. The 2x YPDA that rinsed the 2 L flask was used to re-suspend the pelleted mated cells. The resuspended pellet was pelleted again at 1000x*g* for 10 minutes. The pellet was resuspended in 10 mL of 0.5x YPDA which gave a final volume of 12.2 mL. Ten microliters of mated cells were serially diluted (1:10, 1:100, 1:1000, 1:10000) then plated on DDO media and incubated for 3 days at

30°C to calculate the mating efficiency. Two hundred microliters of the mated cell suspension were plated on every QDO plate (150 x 15 mm size) until all of the suspension had been plated. The mated cells plated on QDO were incubated at 30°C for 72 hours. All formed colonies were transferred to secondary QDO plates. After another 72 hours, any new colonies on the primary QDO plates were also transferred to secondary QDO plates.

Interaction Strengths

The protein interaction strengths of the colonies that resulted from the mating were tested by streaking onto X-α-gal plates. All colonies from the secondary QDO plates and a positive and negative control were streaked onto a tertiary QDO plate and also onto a QDO X-α-gal plate. The plates were incubated at 30°C for 3 days. The blueness produced by each diploid on tertiary QDO X-α-gal plates was ranked on a 0-3 scale. The negative control which had absolutely no growth or blueness served as a marker for 0 and the positive control which resulted in a vibrant blue was used as an example for a ranking of 3 as seen in Figure 7. Any colonies that were given a ranking of less than 1 were not chosen to proceed with plasmid purification.

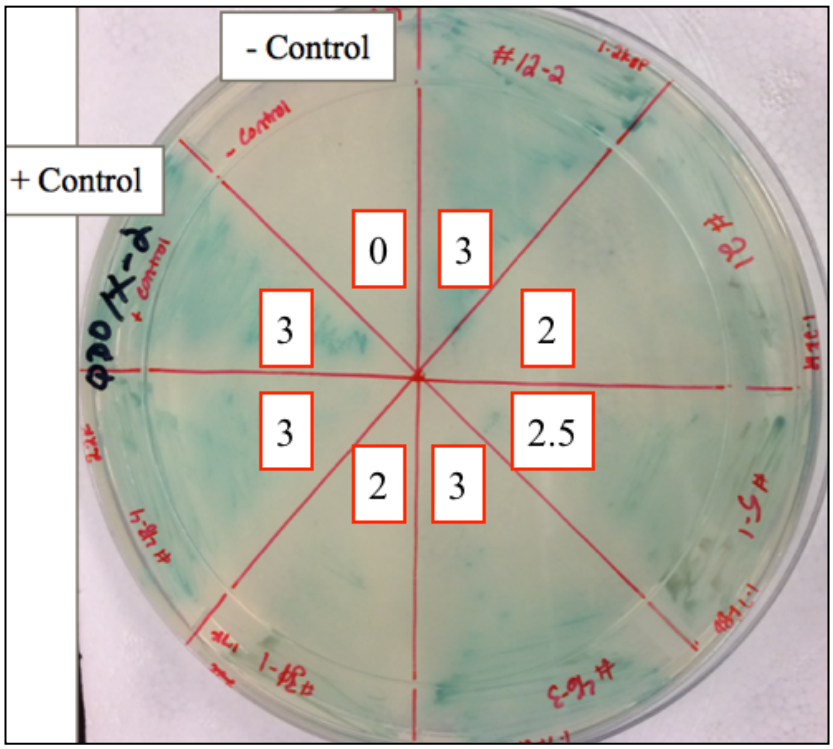

Figure 6: Blue Intensity Ratings. Samples of interacting proteins and positive and negative controls were streaked on X-α-gal plates. The negative control's lack of blue color was used as the marker for a score of 0 and the positive control's strength of blue color as a score of 3. Intensity of blue hues falling in-between 0 and 3 were rated either a 1 or 2. After the number of samples decreased to a more manageable amount, a more descriptive 0-5 rating methodology of blue intensity was used. Ratings for all blue intensities were judged by two individuals; discrepancies were either mediated by giving half-scores or re-evaluation from both individuals. Ratings are shown for each sample above.

Plasmid Purification

The selected colonies were grown by collecting a large pearl sized amount of yeast off of the tertiary QDO plates and suspending in 5 mL of YPD medium. The resuspension was grown at 30°C for 18 hours while shaking at 250 rpm. The overnight grown samples in 5 mL YPD were pelleted in 1.5 mL microfuge tubes by repeated pelleting at 14000x*g* for 10 seconds then decanting. After the samples were pelleted for the last time, 0.2 mL of yeast lysis solution (2% v/v Triton, 1% w/v SDS, 100mM NaCl, 100mM Tris-HCl, 1mM EDTA), 0.2 mL of phenol-

chloroform-isoamyl alcohol and 0.3 g of acid washed glass beads resuspended each pellet and lysed the cells. Then the samples were spun by a vortex for 2 minutes each. The samples were centrifuged at 14,000x*g* for 5 minutes, leaving the DNA in the supernatant. The supernatant was transferred to a new 1.5 mL tube and the DNA was precipitated by adding 34 µL of 3 M NaOAc and 850 µL of ethanol then centrifuging at 14000x*g* for 10 minutes. The supernatant was discarded and the DNA pellet was washed in 1 mL of 70% ethanol. The pellet was centrifuged at 14000x*g* for 10 minutes and was allowed to dry. The resulting DNA pellet was resuspended in 50 mL of TE buffer.

From the crude plasmid purification from yeast, 10 µL of each sample was combined with 100 µL of DH5α competent cells. The plasmids and cells were incubated together on ice for 30 minutes then heat shocked at 42°C for 30 seconds then incubated on ice for another 5 minutes. Afterwards, 890 µL of SOC was added to all samples which were then incubated at 37°C for one hour while shaking at 250 rpm. The transformed cells were then plated in serial dilutions on LB plates containing ampicillin to select for the prey plasmid overnight. An IBI mini prep kit was used to isolate the plasmids from all successful transformations which were analyzed for concentration and purity using Nanodrop2000 equipment.

HindIII **Digest and Gel Electrophoresis**

From all purified plasmid samples, 500 ng of plasmid DNA was digested with *HindIII* for at least one hour. The digested DNA was stained with EasyVision One dye and ran at 150 V in a 1% (w/v) agarose gel with 0.5x TBE buffer for a minimum of 90 minutes. After all samples were digested and ran in electrophoresis gels, band sizes from all inserts were recorded which grouped inserts into categories for size. Additional samples were digested with *HindIII* and

electrophoresed in 2% (w/v) agarose gels at 100 V to identify small bands (<700 base pairs) to further separate samples into protein categories.

Retransformation and Interaction Strength Testing

Individual samples from each insert size group were transformed into strain Y2HGold containing the bait plasmid. Transformed cells were selected for by plating on DDO media. After colony formation after three days, the transformed cells were re-streaked on QDO media containing X-α-gal. The resulting blue intensity of the colonies were rated on a more descriptive scale of 0 to 5, instead of 0 to 3. The re-transformation and blue intensity ratings were replicated with additional samples from each protein category to distinguish if there were different categories of proteins that were grouped into the same category initially.

Sequencing

Eighteen samples total from ten different categories were chosen to sequence. The 18 samples were chosen based on how many samples were in each category, strength of interactions and purity of samples and were sent to the University of South Florida for sequencing. Alignments of sequences and consensus sequences were generated in SeqManPro from DNASTAR bioinformatic software. The resulting consensus sequences were used in BLASTn searches in the toxodb.org database. The sequenced samples were aligned with the full sequence provided from the toxodb.org database to analyze what proportion of the ORF of the full sequence was included in the cDNA library which interacted with Cyc6.

False Positive Testing

A sample from each contig group and each lone sample from the sequencing results were transformed along with the negative control, pGBKT7-lam, into Y2HGold. Transformed cells

and Y2HGold strain positive and negative controls were plated on DDO plates then streaked onto X-α-gal QDO plates at 30°C for 3 days each. False positives were indicative of formation of blue colonies in comparison to the controls.

Selection of TGME49_285160

The sequence of TGME49_285160 was selected to test against Cyc6 due to similarities between other CDKs found in other Eukaryotic phyla. TGME49_285160 was selected due to no previous research being done on this protein relating to any screens or it being the resulting interacting partner of any known screens and due to its strong similarities to human CDK 14, CDK 16 and Eip63E found in *Drosophila melanogaster*. The apparent absence of TGME49_285160 during the tachyzoite life stage (toxodb.org; Alvarez & Suvorova, 2017) implied the yeast two hybrid system did not test this interaction. Selection criteria was based on the E scores obtained when the amino acid residue sequence was used in a BLAST search in a *T. gondii* genome database; the results of which are shown in Tables 1, 2 and 3. While other proteins had lower E-values, such proteins were already the subjects of other screens or directly tested with Cyc6 from previous studies.

Table 1: BLASTp Query of Human CDK14. The FASTA sequence for Human CDK14 was provided by the UniProt database. The sequence was queried in the ToxoDB BLASTp feature. The top five hits are shown.

ToxoID	Predicted Product	Score	E-Value
TGME49_218220	CDK	285	1E-92
TGME49_285160	CDK5	208	4E-62
TGME49_304970	CDK	206	2E-57
TGME49_281450	CDK	189	3E-54
TGME49_233010	ERK7	163	5E-44

Table 2: BLASTp Query of Human CDK14. The FASTA sequence for Human CDK16 was provided by the UniProt database. The sequence was queried in the ToxoDB BLASTp feature. The top five hits are shown.

ToxoID	Predicted Product	Score	E-Value
TGME49_218220	CDK	326	6E-108
TGME49_304970	CDK	202	1E-55
TGME49_285160	CDK5	198	4E-58
TGME49_281450	CDK	194	8E-56
TGME49_233010	ERK7	184	7E-51

Table 3: BLASTp Query for *Drosophila* Eip63E. The FASTA sequence for *Drosophila melanogaster* Eip63E was provided by the UniProt database. The sequence was queried in the ToxoDB BLASTp feature. The top five hits are shown.

ToxoID	Predicted Product	Score	E-Value
TGME49_218220	CDK	280	1E-89
TGME49_304970	CDK	190	1E-51
TGME49_285160	CDK5	188	2E-54
TGME49_281450	CDK	181	9E-51
TGME49_233010	ERK7	169	1E-45

TGME49_285160 Testing

The DNA sequence for TGME49_285160, with restriction sites for *NdeI* and *EcoRI* located at the 5' and 3' ends respectively, was purchased through BioMatik in vector, pBluescript II SK. NEB DH5-alpha *E. coli* were transformed with 100 ng of the pBluescript plasmid and 100 ng of the positive control, puc19, and plated on LB-amp (50 μg/mL). Untransformed cells served as the negative control. After incubating overnight at 37°C, 3 colonies containing pBluescript-TGME49_285160 were inoculated in 5 mL of LB liquid media containing 50 μg/mL ampicillin at 37°C while shaking at 250 rpm and harvested when $OD_{600nm} > 1.2$. An IBI mini prep kit was used to purify the plasmids. The yield was determined with Nanodrop 2000 equipment.

TGME49_285160 Subcloning. The TGME49_285160 insert was removed from pBluescript by NEB *EcoRI HF* and *NdeI* digestion of 1 μg of DNA at 37°C for two hours. Simultaneously, 1 μg of empty pGADT7 vector was digested by the same process for one hour. The pGADT7 digest was heat shocked at 65°C for 20 minutes to inactivate the restriction enzymes. The digested pGADT7 vector was cooled down to 37°C and then was incubated with 1 unit of NEB rSAP for 30 minutes. Twenty microliters of products from both digests were stained with EZ-Vision One dye and ran at 150 V in a 0.5x TBE 0.8% (w/v) agarose gel for varying lengths of time. The bands of the insert and linearized vector were excised from the gel after the representative bands had travelled at least 2/3 of the way down the 15 cm long agarose gel to ensure only digested vector DNA would be purified. The bands representing the insert and linear vector were excised from the agarose gel in quantities < 500 mg. The DNA was purified using an IBI DNA fragment extraction kit and quantified. A 3:1 molar ratio of insert to vector was used

for ligation, respectively. Four hundred units of NEB T4 DNA ligase was incubated with 100 ng of vector DNA and 37.5 ng of insert DNA at 20°C for 10 minutes. The reaction was chilled on ice then used to transform 50 uL of NEB DH5α *E. coli* cells following the NEB transformation protocol. Serial dilutions of 1:1 to 1:1000 of transformed cells were plated on LB agar containing 50 μg/mL ampicillin selecting for successfully transformed cells. After incubation at 37°C overnight, transformation efficiency was calculated and three colonies were inoculated in 5 mL of LB liquid media containing 50 μg/mL ampicillin and were harvested when $OD_{600nm} > 1.2$. The plasmid DNA was purified using an IBI miniprep kit and quantified. The successful ligation of insert and pGADT7 was confirmed by performing a double restriction enzyme digest with NEB *EcoRI HF* and *NdeI* of pGADT7 with the TGME49_285160 insert and of an empty pGADT7 vector. The products of each digestion were stained with EZ Vision One dye and ran on a 0.5x TBE, 1.2% (w/v) agarose gel at 150 V alongside a 1kb ladder for 120 minutes. The resulting fragment sizes confirmed successful ligation of the insert into pGADT7 represented by two respective bands.

TGME49_285160 & TGME49_266900 Interaction Tests. Three Y2HG colonies, approximately 2-3 mm in diameter, grown on agar YPD media were inoculated in 50 mL of YPD liquid media at 30°C while shaking at 250 rpm overnight. When the culture reached stationary phase ($OD_{600nm} > 1.5$), the cells were harvested and transformed with pGADT7-TGME49_285160 following the same protocol used for Y2HG cells and the pGBKT7-Cyc6 transformation. Successful transformations were selected by plating transformed yeast in serial dilutions of 1:1 to 1:10000 on leucine dropout media at 30°C for three days. Three of the larger colonies were inoculated in liquid leucine dropout media overnight at 30°C while shaking at 250 rpm and

harvested when OD_{600nm} >1.5. To select for transformed cells containing both plasmids, the cells were plated on DDO for three days at 30°C in serial dilutions of 1:1 to 1:10000.

Colonies which contained both plasmids were streaked onto QDO agar plates. Additionally, positive control pGBKT7-p53 + pGADT7-T antigen and negative control pGBKT7-lam + pGADT7-T antigen were used to validate findings. After incubating for three days at 30°C, the presence or absence of colonies was noted.

To guarantee both inserts were present in the co-transformed colonies, PCR amplified both Cyc6 and TGME285160 inserts from their respective plasmids. The primers used to sub-clone Cyc6 from pGADT7 to pGBKT7 and the T7 and 3' AD sequencing primers from Clontech were used to amplify the co-transformed yeast. As a positive control, Cyc6 and TGME49_285160 inserts were amplified from their respective plasmids.

Chapter IV: Results

Overview

From this current yeast two hybrid screen, two likely protein interactions were identified with Cyc6: TGME49_214290 and TGME49_314890. Three proteins consisting of a ribosomal protein and two GRA proteins were identified and deemed to be false positives. Three other interacting proteins were classified as hypothetical proteins which had no conserved domains or well-aligned expression rates in life stages or cell cycle phases with Cyc6. When Cyc6 was directly tested with TGME49_285160, no protein-protein interaction was observed.

Subcloning and Transformation

Successful subcloning of the Cyc6 insert was evident by the lengths of DNA bands in an electrophoresis gel corresponding to the expected sizes of a *HindIII* digest of pGADT7 and pGBKT7 both containing the Cyc6 insert as shown in Figure 7.

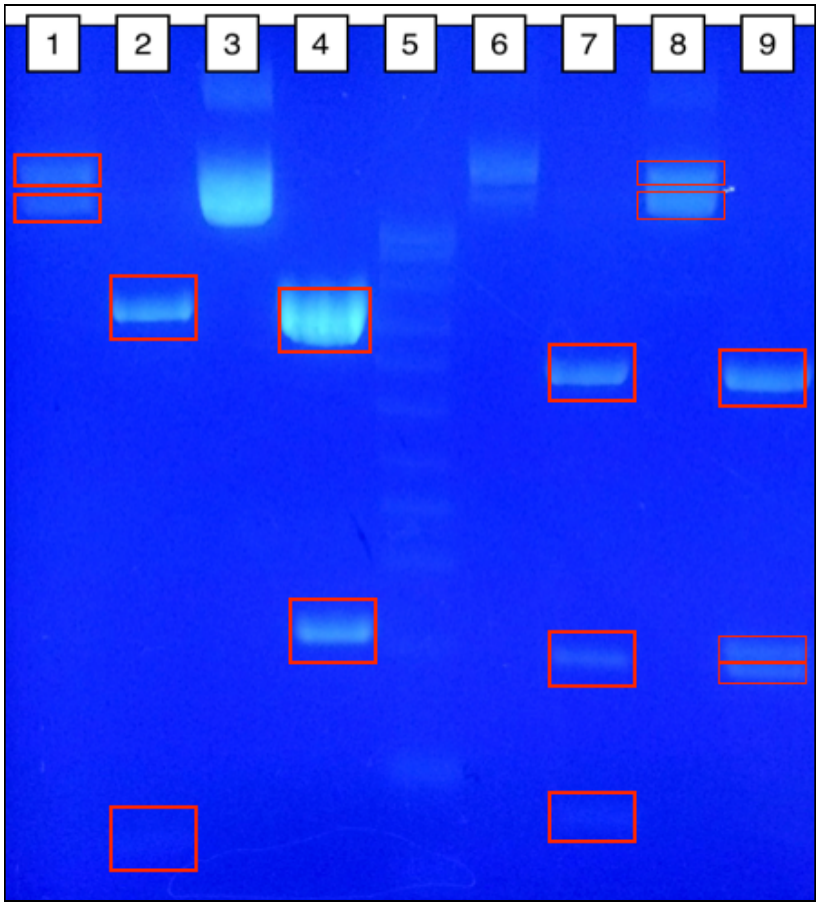

Figure 7: Subcloning of Cyc6 Insert. Successful subcloning of Cyc6 from pGADT7 to pGBKT7 is shown in an 1% (w/v) agarose gel. The contents of lanes 1 to 9 contain uncut empty pGADT7, empty pGADT7 digested with *HindIII,* uncut pGADT7-Cyc6, pGADT7-Cyc6 digested with *HindIII*, 1 kb ladder, uncut empty pGBKT7, empty pGBKT7 digested with *HindIII,* uncut pGBKT7-Cyc6 and pGBKT7-Cyc6 digested with *HindIII*.

Auto-activation Testing

Cyc6 was shown to not interact with the negative control (pGADT7-lam) as indicated by lack of growth on QDO. This indicates that Cyc6 is not a "sticky" protein. Y2HGold cells with only the bait plasmid indicated Cyc6 did not auto-activate when streaked on media lacking histidine and tryptophan as indicated by lack of growth.

Yeast Two Hybrid System Outcome Overview

The bait strain had a viability of $7.3x10^7$ cfu/mL and the prey strain had a viability of $3.1x10^7$ cfu/mL. The mating efficiency of the yeast two hybrid system was $3.2x10^6$ cfu/mL, or $3.9x10^7$ diploids total. The yeast two hybrid system produced 95 colonies of diploid cells containing proteins interacting with Cyc6 from the $3.9x10^7$ diploids. After excluding all samples that did not produce a blue color rating of 1 or greater when grown on QDO X-α-gal plates, the number of viable samples decreased to 80 (Table 4). Of the 80 samples, 76 plasmids were able to be purified and transformed into *E. coli*.

Table 4: Intensity of Blueness Rating Frequencies. Shown below are the frequency of interaction strength ratings from original 95 colonies. The 15 samples that produced blue intensities with a rating of less than one were excluded.

Rating	# of Colonies
<1	15
1	15
2	26
3	39

Protein Groupings

Of the 76 plasmids, 70 were able to be visualized in 1% (w/v) agarose gels. The six plasmids that were unable to be seen in the agarose gel had significantly less DNA yield after purification or had A260/230 ratios that were significantly lower than other purified samples which suggests organic contamination from a previous step. After the initial digest and 1% (w/v) agarose gel electrophoresis, six different groups of proteins were apparent (Table 5).

Table 5: Initial Six Protein Groups. The initial grouping of proteins from 1% (w/v) agarose gels is described below. When yeast were re-transformed with multiple samples from each category then ran *HindIII* digested plasmids on 2% (w/v) agarose gels, this table was shown to be inaccurate due to inconsistencies seen in interaction strength and inserts.

Fragment(s) bp	Insert Length bp	# of Samples
1.2k	400	9
1.7k	900	5
2k	1.2k	7
2.4k	1.6k	34
2.6k	1.8k	13
1.2k, 800	1.2k	2

After retransforming back into yeast, five of the six groups had discrepancies in interaction strength ratings when grown on X-α-gal media. The secondary digests and electrophoresis on 2% agarose gels (Figure 8) provided evidence of 10 groups of proteins instead of only six which was distinguishable by differences in base pair amounts (Table 6). To find the length of just the insert, 800 bp was subtracted from the total length of each insert due to 800 bp separating the two *HindIII* sites in the pGADT7 vector. Additionally, a few samples had multiple fragments which suggests there was a *HindIII* site in the insert. Although the new grouping of proteins allowed for a consensus for most protein groups and interaction strength rating, two inserts (fragment lengths of 2k bp and 2.4k bp) did not have a distinguishable size difference, but produced two different interaction strengths with two of its corresponding samples.

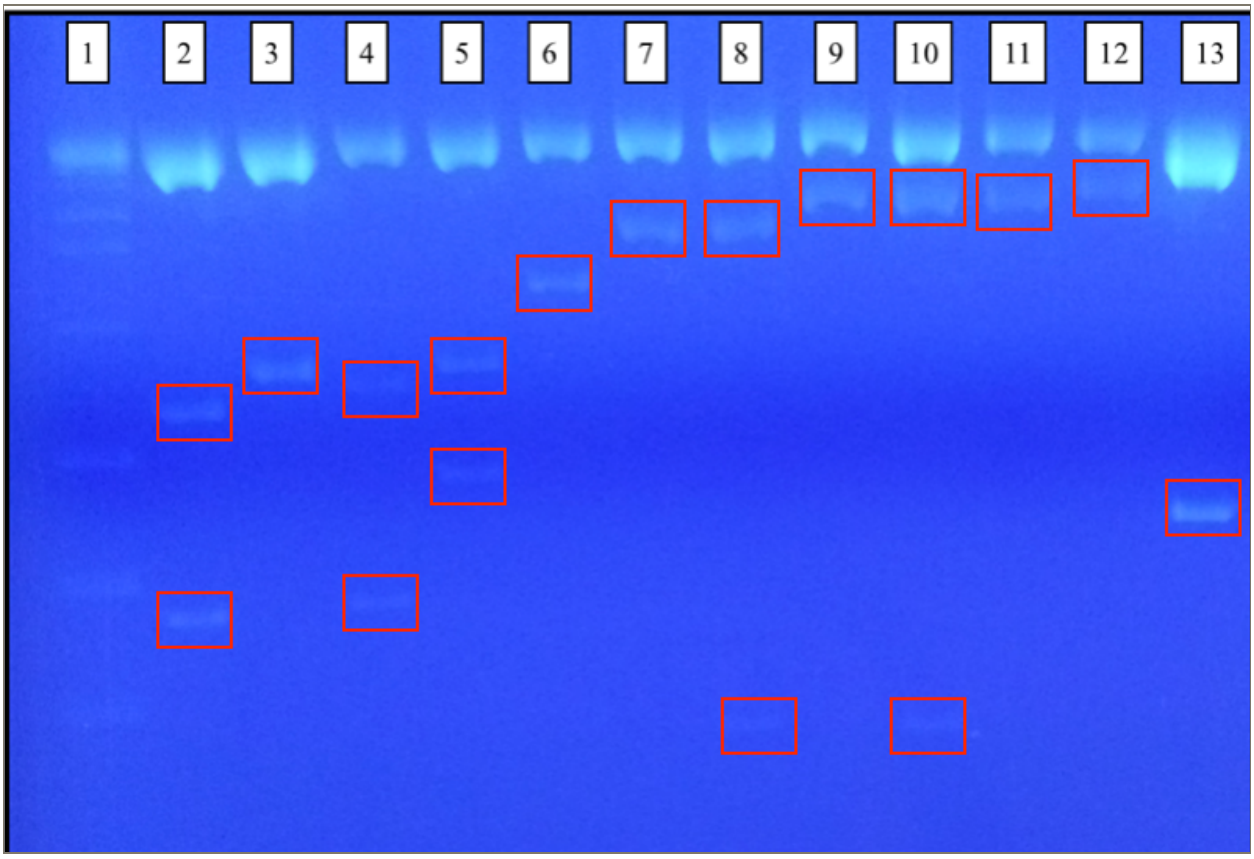

Figure 8: Protein Categories by Insert Length. All 10 inserts were digested with *HindIII* and electrophoresed on a 2% (w/v) agarose gel. The 13 lanes from left to right consist of: 1 kb ladder, inserts of 1.1k + 650 bp, 1.3k bp, 1.2k + 700 bp, 1.3k + 900bp, 1.7k bp, 2k bp, 2k + 400 bp, 2.4k bp, 2.4k + 400 bp, 2.4k bp and 2.6k bp in length, and empty pGADT7 digested with *HindIII*, respectively. Lanes 9 and 11 could not be distinguished apart by size, but were from samples with different interaction strengths.

Table 6: Frequencies of Insert Lengths and Blue Intensity Ratings. Fragment lengths shown in column one correspond to the total length of the bands seen in a 2% (w/v) agarose gel before 800bp was subtracted and any bands with multiple fragments were added together to get the total length of the insert. *These inserts could not be distinguished by size, but produced significantly different interaction strength ratings.

Fragment Length(s) (bp)	Actual Insert Length (bp)	# of Samples	Interaction Strength(s) (1-5)
1.1k, 650	950	2	3
1.3k	500	5	5
1.2k, 700	1.1k	1	5
1.3k, 900	1.4k	1	2
1.7k	900	5	4
2k	1.2k	7	1, 5*
2k, 400	1.6k	1	1.5
2.4k	1.6k	40	2, 5*
2.4k, 400	2k	4	1
2.6k	1.8k	4	5

Interacting Proteins. After the all samples were categorized into one of the 10 possible groups and a representative 18 samples were sequenced, nine different interacting proteins were evident. From the 18 samples sequenced, five different contigs and four lone samples without contigs were aligned using the SeqManPro program from DNASTAR bioinformatic software as seen in Table 7.

Table 7: Contig Alignment and Insert Identification. Shown below are each of the contigs and lone sequences. After aligning, each contig or sequence was located in the Toxodb database by a BLASTn search. Each query generated one hit with an E-value of 0. The samples above in red boxes indicate biologically relevant relevant proteins.

Contig #	# of Sequences	Insert Length (bp)	Interaction Strength (1-5)	ToxoID (TGME49_#)	Predicted Protein Product	# of Amino Acids
1	2	2k	2.5	215220	GRA22	629
2	2	1.2k	1	226570	Hypothetical	139
3	2	1.4k	2.5	203358	Hypothetical	395
4	2	400	2	286450	GRA5	120
5	7	1.6k	5	-	-	-
Single 1	1	2.6k	5	266690	Hypothetical	1676
Single 2	1	1.6k	2	314890	ThiF Protein	2933
Single 3	1	1.1k	5	320050	Ribosomal RLP5	310
Single 4	1	900	5	214290	DJ-1 Family Protein	256

Sticky proteins formed the largest contig (contig #5) and were excluded from further analysis. In total, eight different proteins were discovered to interact with Cyc6, excluding the sticky protein, from the yeast two hybrid screen. The degree of interaction strength of the proteins and Cyc6 varied from 1 to 5 on a scale of 0 to 5 rating the intensity of the blue color produced from X-α-gal.

TGME49_285160

Strain Y2HGold was co-transformed with pGBKT7-Cyc6 and pGADT7-TGME49_285160. Evidence of successful co-transformation was shown by growth on DDO media (Figure 9) and PCR amplification of the inserts directly from yeast (Figure 10) which correspond with the expected insert sizes. No growth of this co-transformed yeast was observed

on QDO (Figure 11) which indicated no interaction between Cyc6 and TGME49_285160 occurred.

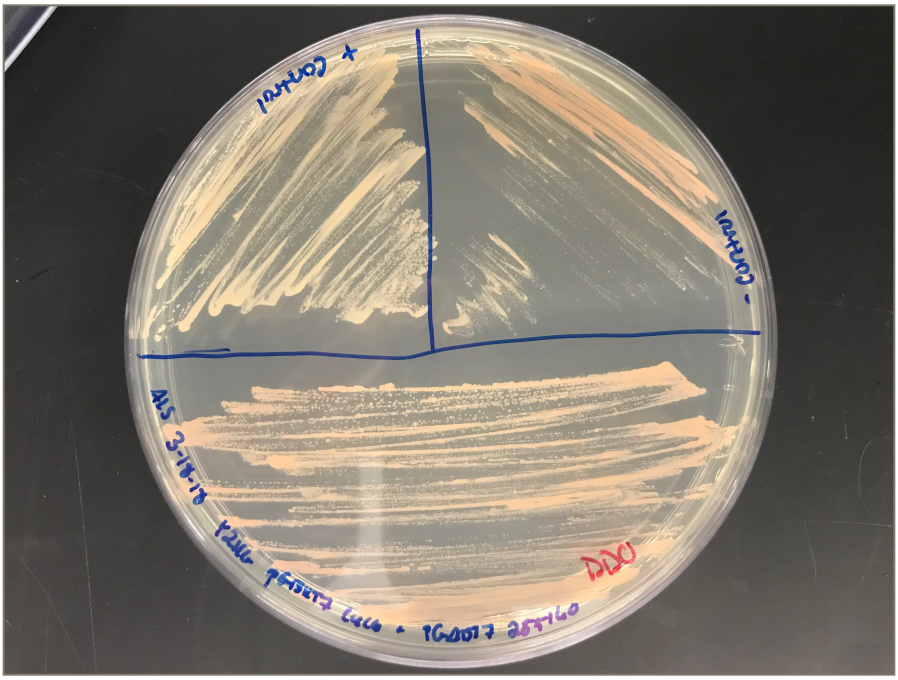

Figure 9: TGME49_285160 Co-transformation. Growth on DDO of co-transformed Y2HGold with pGBKT7-Cyc6 and pGADT7-TGME49_285160 is evident on the bottom section. Positive and negative controls are evident on the top left and right sections, respectively.

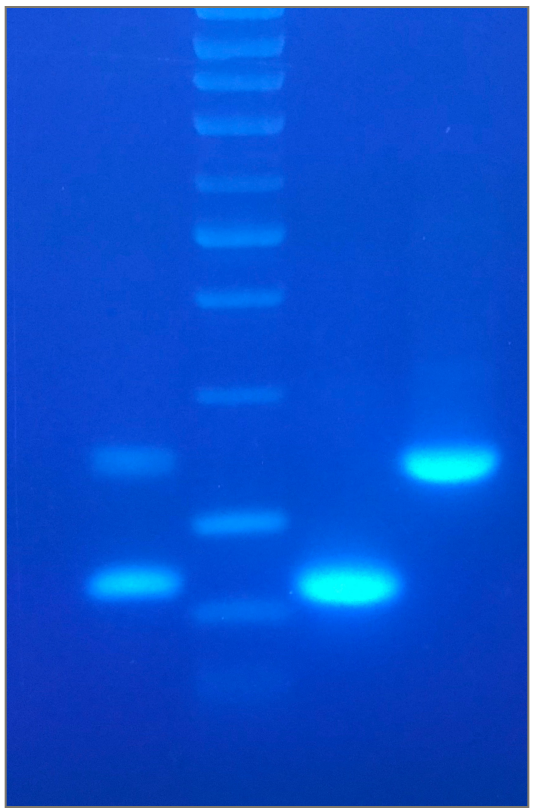

Figure 10: Affirmation of Presence of TGME49_285160 Insert. The two inserts of Cyc6 and TGME49_285160 (Lane 1) were amplified from yeast grown on DDO to further indicate successful transformation with the original primers used for sub-cloning Cyc6 into pGBKT7 and the T7 and 3'AD sequencing primers. Lane 2 represents a 1 kb ladder, Lane 3 is the Cyc6 insert from pGBKT7 amplified by the original primers used for sub-cloning and Lane 4 is the TGME49_285160 insert amplified from pGADT7 by the T7 & 3' AD sequencing primers provided by Clontech.

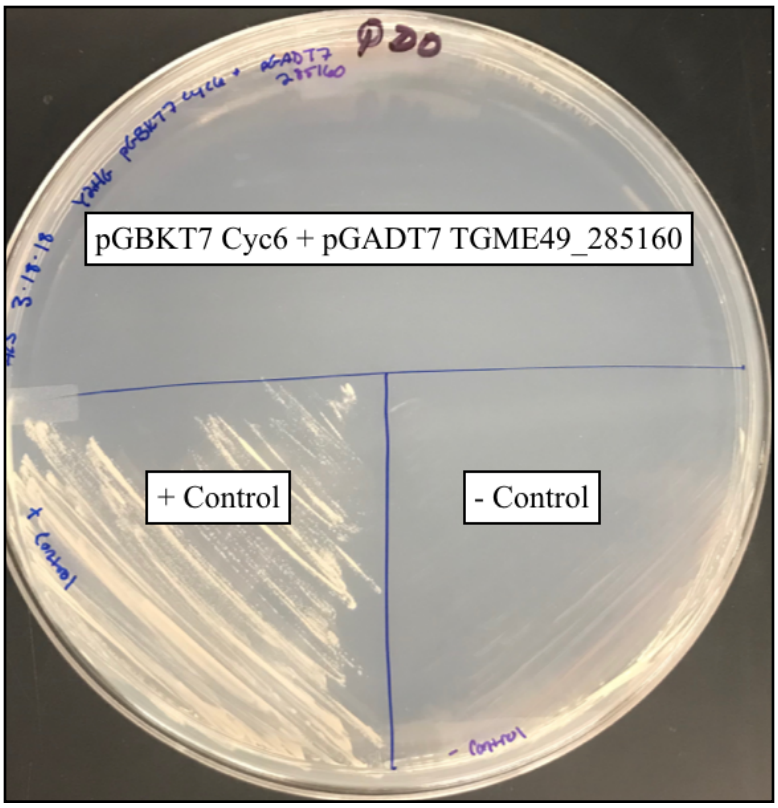

Figure 11: Cyc6 and TGME49_285160 Interaction Testing. No growth was observed on QDO media with yeast co-transformed with pGBKT7-Cyc6 and pGADT7-TGME49_285160. Growth was observed with the positive control as seen in the lower left section and no growth occurred with the negative control in the lower right section.

Chapter V: Discussion

Interacting Proteins

Although only two proteins were able to be classified as Cyc6 interacting proteins with a high degree of certainty, six other proteins were excluded from analysis due to various reasons, such as their respective intracellular location within *T. gondii*, and lack of homologous expression in specific life stages. Despite TGME49_285160 sharing a high degree of homology with other Cyc Y interacting CDKs from other eukaryotes, no interaction was observed. The insert lengths of each interacting protein sequence were compared to the complete protein sequence from the toxodb.org database to analyze where Cyc6 interacts with each protein (Figure 12). No significant similarities between the DJ-1, ThiF or hypothetical proteins were found by BLASTp alignment. The span of the interacting cDNA of the hypothetical proteins are shown in Figure 13.

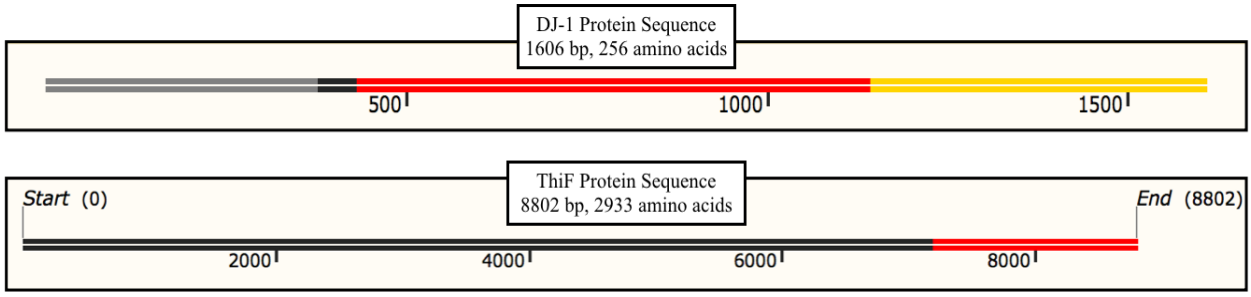

Figure 12: Insert Alignments and Locations in Sequences of Biologically Relevant Interactions. The span of the interacting cDNA inserts are shown above in proportion to the entire insert sequence length. The red fractions represent ORFs and the yellow fractions represent UTRs included in the interacting cDNA insert. The black and grey fractions represent the ORFs and UTRs, respectively, not included in the interacting cDNA insert.

The proportion of cDNA coverage of the ORF region between the DJ-1 and ThiF protein sequences varies due to the differing ORF lengths. The insert length corresponding to DJ-1 was

900 bp which provided all but the first 60 bp of the ORF (the first 20 amino acids) out of the 256 amino acid protein length. However, the ThiF insert only covered approximately the last 533 amino acids out of a total length of 2933 amino acids. The ORFs included in the interacting cDNA inserts of DJ-1 and ThiF did not align in NCBI's BLASTn program.

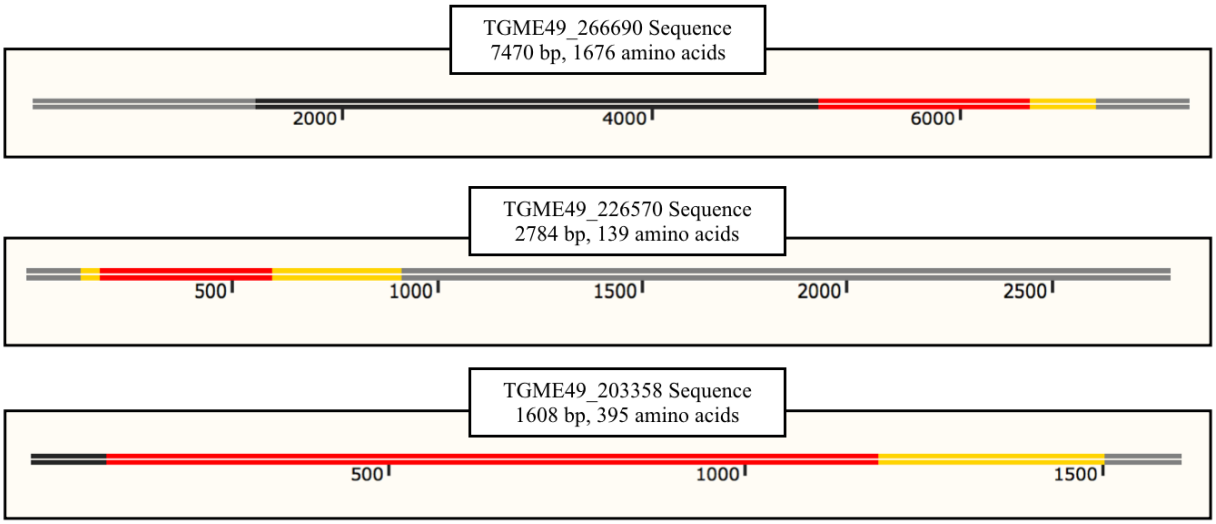

Figure 13: Insert Alignments and Locations in Sequences of Hypothetical Proteins. The three hypothetical proteins are shown above with the same colors representing the ORFs and UTRs included in each cDNA insert. The ORFs and UTRs not included in the cDNA insert are shown in black and grey, respectively.

Although it is unknown if the three interacting hypothetical proteins pulled from this screen exist in vivo, the entire predicted ORF of TGME49_226570 and most of TGME49_203358's ORF were included in interacting cDNA inserts. A lesser proportion of TGME49_266690's ORF was included, but the corresponding insert length was a considerable 1.8k bp long. No significant alignments were found when comparing the hypothetical, DJ-1 and ThiF sequences together in the NCBI BLASTn suite. Therefore, no common motifs or domains existed between the interacting proteins that had a role in Cyc6 interactions.

TGME49_214290. One distinct protein as a Cyc6 interacting partner was identified as TGME49_214290, a DJ-1 family protein. More specifically, this protein in *T. gondii* has an apparent role in microneme secretion. Previous research suggests DJ-1 functions as a "noncanonical kinase-regulatory scaffold" and is necessary for successful *T. gondii* microneme secretion. This DJ-1 protein has been shown to have a direct interaction with a calcium dependent kinase, which microneme secretion is reliant on (Child et al., 2017). It is unknown what Cyc6's role regarding DJ-1 function or vice versa, but it is easy to speculate Cyc6 may play a role in a pathway allowing for microneme secretion.

TGME49_314890. The other interacting protein partner of Cyc6 was TGME49_314890, a ThiF protein, similar to E1 enzymes in the Eukaryotic ubiquitination pathway. The ThiS-ThiF protein complex has been described in *E. coli* to allow the transfer of sulfur for thiazole biosynthesis in the overarching thiamin biosynthesis pathway (Lehmann, Begley & Ealick, 2006). Cyc6 may play a role in the ubiquitination pathway of specific proteins perhaps allowing the parasite to transition into the bradyzoite life stage. However, it is important to note that such protein-protein interactions must be studied in greater detail in order to draw conclusions about Cyc6's role in its interaction with the ThiF protein.

Excluded Interacting Inserts

From the nine interacting inserts after sequence alignment, seven were excluded. When deciding which results were false positives, the limitations of the yeast two hybrid system were considered. The first sequence to be excluded was a promiscuous protein that produced blue colonies similar to the positive control when strain Y2HGold was co-transformed with pGBKT7

lam and pGADT7 containing the insert from contig #5. Due to the lack of specificity of this protein, it was considered a false positive.

One main critique of the yeast two hybrid system is the possibility of obtaining false positives of proteins that do interact in this system in a non-promiscuous manner, but that would not interact in *T. gondii* itself, perhaps due to the inconsistent localization of these proteins observed naturally in *T. gondii*. A ribosomal protein, RPL5 (TGME49_320050), was excluded due to the localization of this protein compared to Cyc6. Since RPL5 is localized in the ribosome, it does not seem feasible based on biological sense that this is a real result. Two other proteins, GRA5 and GRA22 (TGME49_286450 & TGME49_215220) are described in previous literature as dense granule proteins (cite). While it is possible Cyc6 may exit the nucleus upon *T. gondii* transitioning from tachyzoite to bradyzoite, GRA5 and GRA22 are located within the parasitophorous vacuole membrane, which is outside of the cell thus separated from Cyc6.

Absence of Interaction with TGME49_285160

No interaction was observed with putative CDK TGME49_285160. Interestingly, this putative CDK does not have any cyclin partners described yet in previous research but is listed as a CDK Family 5 protein on toxodb.org due to conserved CDK specific domains identified by InterPro, a database for protein families, domains and functional sites (Finn et al., 2017). It is possible that Cyc6 interacts with a CDK expressed in greater proportions in the bradyzoite life stage compared to the tachyzoite life stage, but it can be concluded that TGME49_285160, a putative CDK with this quality, does not interact with Cyc6.

Limitations

The yeast two hybrid system is an efficient and reliable method for scanning transcriptomes for protein-protein interactions. This current study generated valuable information regarding Cyc6's protein interactions, or lack of. Even though no CDK partner was found, the existence of a CDK interacting with Cyc6 in a biologically real environment cannot be disproven. Additionally, there may be a variety of other proteins interacting with Cyc6 that were not evident from the yeast two hybrid screen. One limitation is the 3' end bias of inserts from the cDNA library. Oligo-dT primers were used in the initial creation of the cDNA library which implies there is a bias towards the C-terminus end of *T. gondii* proteins and in many cases, the N-terminus may not have been included in the screen. As shown in Figure 12, the majority of the coding region for the ThiF protein is excluded, but according to the insert length and sequence alignment, Cyc6 interacts with a region towards the C-terminus of the ThiF protein. Due to the 3' end bias, several proteins that have an N-terminus interaction with Cyc6 may not have been accounted for in this current screen. One suggestion to fix this limitation would be to include random hexamer primers when creating a cDNA library (Cash, 2016). When testing TGME49_285160, this limitation did not need to be considered as the entire transcript was tested.

Conclusions

It was hypothesized that Cyc6 would interact with a CDK either found from the yeast two hybrid screen or by a direct co-transformation of Y2HGold strain of *Saccharomyces cerevisiae* of both protein sequence inserts in their respective plasmids. No CDK partners, experimentally verified as CDKs or putative CDKs were found to interact with putative cyclin, Cyc6. This leads

to the question of whether Cyc6 even has a CDK partner, or perhaps Cyc6 plays a noncanonical role in other functions of *T. gondii*. However, it is possible a CDK partner does exist for Cyc6 due to certain limitations of this current study, but there is no substantial evidence to support the existence of a CDK partner.

Despite the lack of evidence of a CDK partner, two biologically relevant proteins were found to interact with Cyc6: a DJ-1 protein and a ThiF protein. Any further analysis about these interactions will need further research to determine Cyc6's role in these interactions. However, if Cyc6 does play a role with DJ-1 and microneme secretion, an area of potential investigation could involve disruption of this interaction to prevent host cell invasion. If the parasite is unable to properly invade a host cell, it may remain an immunogenic target and would lose its Trojan Horse like mechanism of discreetly residing in host cells to allow its transportation into distant host cell tissues, such as the brain. Similar to the 2017 study done by Child et al., the interaction of Cyc6 and DJ-1 could be interrupted either by a molecular blocker or by creating a Cyc6 knockout strain then measuring the impact, if any, by quantifying the secretion of proteins specific to micronemes, such as MIC proteins. On the other hand, examining the role of Cyc6's interaction with a ThiF protein may be more complicated as there is little research regarding ThiF proteins in *T. gondii* compared to DJ-1 proteins and their interactions with calcium dependent kinases and microneme secretion. If the ThiF protein pulled from this screen is found to play a role in the ubiquitination pathway of specific proteins, the question of Cyc6's involvement in this process can be investigated in a few ways. One potential experiment could involve blocking the interaction of Cyc6 and the ThiF protein, then monitor any changes in the amount of proteins present in the cell compared to wild type *T. gondii*. If Cyc6 does play a role in

differentiation to the bradyzoite life stage, Cyc6 could serve as a necessary component in the ubiquitination pathway of proteins specific to the tachyzoite life stage.

Although this current study only could confirm two Cyc6 protein interactions and not provide further conclusive data into Cyc6's involvement in cellular processes in *T. gondii*, the information generated creates several important questions that may lead to great advances in better understanding this enigmatic parasite. Although TGME49_285160, a putative CDK, did not interact with Cyc6, this poses another mystery: if Cyc6 was a protein of interest due to lack of an interacting CDK partner, the same could be said for a putative CDK without an interacting cyclin partner. To date, no research has found a cyclin that interacts with TGME49_285160, or has attempted to. TGME49_285160 has been classified as a CDK family 5 type of protein (toxodb.org), but if this annotation based on bioinformatic software is correct, this would imply that a cyclin must interact to allow this putative CDK to phosphorylate its target substrate. Therefore, future research should examine this "orphan" CDK to either find a cyclin partner or classify this protein as another type of kinase.

The aim of this study was to identify protein-protein interactions with putative cyclin, Cyc6. While a few protein partners were found, the lack of certain interactions further generates information about this putative cyclin. While it cannot be concluded with certainty Cyc6 does not have a CDK partner, this research continues the elimination of potential interacting CDK partners which may lead to a stronger focus on noncanonical cyclin functions, of which may play a crucial role in allowing *T. gondii* to be a notoriously successful parasite.

References

Ajzenberg, D., Bañuls, A., Tibayrenc, M. & Dardé, M. L. (2002). Microsatellite analysis of *Toxoplasma gondii* shows considerable polymorphism structured into two main clonal groups. *International Journal for Parasitology, 32*, 27-38.

Alvarez, C. A., & Suvorova, E. S. (2017). Checkpoints of apicomplexan cell division identified in *Toxoplasma gondii*. *PLoS Pathogens*, *13*(7), e1006483. http://doi.org/10.1371/journal.ppat.1006483.

Andrews, B. & Measday, V. (1998) The cyclin family of budding yeast:abundant use of a good idea, *Trends in Genetics 14*(2), 66-72, ISSN 0168-9525, https://doi.org/10.1016/S0168-9525(97)01322-X.

Behnke, M. S., Wootton, J. C., Lehmann, M. M., Radke, J. B., Lucas, O., Nawas, J., Sibley, L. D. & White, M. W. (2010). Coordinated progression through two subtranscriptomes underlies the tachyzoite cycle of *Toxoplasma gondii. PLoS ONE, 5*(8), e12354. http://doi: 10.1371/journal.pone.0012354.

Cash, B. (2016). "TgRCC1IV and AP2VIII-3 Are Putative Interactors of Organellar Division Protein ECR2 in *Toxoplasma gondii*." *Culminating Projects in Biology*. 15. Retrieved from: http://repository.stcloudstate.edu/biol_etds/15.

Child, M., Garland, M., Foe, I., Madezelan, P., Treeck, M., van der Linden, W., Oresic Bender, K., Weerapana, E., Wilson, M., Boothroyd, J., Reese, M. & Bogyo, M. (2017). *Toxoplasma* DJ-1 regulates organelle secretion by a direct interaction with calcium-dependent protein kinase 1. *mBio 8*(1), e02189-16. doi:10.1128/mBio.02189-16.

Dardé, M. L. (2008). *Toxoplasma gondii*, "new" genotypes and virulence. *Parasite, 15*, 366-371.

Davidson, G. & Niehrs, C. (2010) Emerging links between CDK cell cycle regulators and Wnt signaling. *Trends in Cell Biology 20*(4), 453-60. doi:10.1016/j.tcb.2010.05.002.

Dupont, C. D., Christian, D. A. & Hunter, C. A. (2012). Immune response and immunopathology during toxoplasmosis. *Seminars in Immunopathology 34*(6), 793-813. http://doi:10.1007/s00281-012-0339-3.

Dubey, J. P. (1998). Advances in the life cycle of *Toxoplasma gondii*. *International Journal for Parasitology*, *28,* 1019-1024.

Dubey, J. P. & Jones, J. L. (2008). *Toxoplasma gondii* infection in humans and animals in the United States. *International Journal for Parasitology, 38,* 1257-1278. http://doi:10.1016/j.ijpara.2008.03.007.

Eaton, M., Weiss, L. & Kim, K. (2006). Cyclic nucleotide kinases and tachyzoite-bradyzoite transition in *Toxoplasma gondii. International Journal of Parasitology*, *36*(1), 107-114.

Esshili, A., Thabet, S., Jemli, A., Trifa, F., Mechri, A., Zaafrane, F. Gaha, L., Babba, H. & Bel Hadj Jrad, B. (2016). *Toxoplasma gondii* infection in schizophrenia and associated clinical features. *Psychiatry Research, 245*, 327-332. http://dx.doi.org/10.1016/j.psychres.2016.08.056.

Filisetti, D. & Candolfi, E. (2004). Immune response to *Toxoplasma gondii. Annali dell'Istituto Superiore di Sanità, 40*(1), 71-80.

Finn, R. D., Attwood, T. K., Babbitt, P. C., Bateman, A., Bork, P., Bridge, A. J., Chang, H. Y., Dosztányi, Z., El-Gebali, S., Fraser, M., Gough, J., Haft, D., Holliday, G. L., Huang, H., Huang, X., Letunic, I., Lopez, R., Lu, S., Marchler-Bauer, A., Mi, H., Mistry, J., Natale, D. A., Necci, M., Nuka, G., Orengo, C. A., Park, Y., Pesseat, S., Piovesan, D., Potter, S. C., Rawlings, N. D., Redaschi, N., Richardson, L., Rivoire, C., Sangrador-Vegas, A., Sigrist, C., Sillitoe, I., Smithers, B,; Squizzato, S., Sutton, G., Thanki, N., Thomas, P. D., Tosatto, S. C., Wu, C. H., Xenarios, I., Yeh, L. S., Young, S. Y. & Mitchell, A. L. (2016). InterPro in 2017-beyond protein family and domain annotations. *Nucleic Acids Research, 45*(D1): D190–D199. doi:10.1093/nar/gkw1107.

Francia, M. E. & Striepen, B. (2014). Cell division in apicomplexan parasites. *Nature Reviews Microbiology, 12,* 125-135.

Fuller-Torrey, E., Simmons, W. & Yolken, R. H. (2015). Is childhood cat ownership a risk factor for schizophrenia later in life? *Schizophrenia Research, 165*, 1-2. http://dx.doi.org/10.1016/j.scres.2015.03.036.

Gubbels, M., White, M. & Szatanek, T. (2008) The cell cycle and cell division: Tightly knit or loosely stitched? *International Journal for Parasitology, 38*(12), 1343-1358. http://dx.doi.org/10.1016/j.ijpara.2008.06.004

Hill, D. & Dubey, J. P. (2002). *Toxoplasma gondii*: transmission, diagnosis and prevention. *Clinical Microbiology and Infection, 8*(10), 634-640. doi: 10.1046/j.1469-0691.2002.00485.x.

Huang, S., Holmes, M., Radke, J., Hong, D., Liu, T., White, M. and Sullivan, W. (2017). *Toxoplasma gondii* AP2IX-4 regulates gene expression during bradyzoite development. *mSphere, 2*(2) e00054-17. doi: 10.1128/mSphere.00054-17

Jiang, M., Gao, Y., Yang, T., Zhu, X. & Chen, J. (2009). Cyclin Y, a novel membrane-associated cyclin, interacts with PFTK1. *FEBS Letters, 583*, 2171-2178.

Kvaal, C., Radke, J., Guerini, M. & White, M. (2002). Isolation of a *Toxoplasma gondii* cyclin by yeast two-hybrid interactive screen. *Molecular and Biochemical Parasitology 120*(2), 187-194.

Kim, K. (2015). A bradyzoite is a bradyzoite is a bradyzoite? *Trends in Parasitology, 31*(12), 610-612.

Krishnamurthy, S., Konstantinou, E. K. Young, L. H., Gold, D. A. & Saeil, J. P. J. (2017). The human immune response to *Toxoplasma*: autophagy versus cell death. *PLOS Pathogens 13*(3), doi:10.1371/journal.ppat.1006176.

Lehmann, C., Begley, T. & Ealick, S. (2006). Structure of the *Escherichia coli* ThiS-ThiF complex, a key component of the sulfur transfer system in thiamin biosynthesis. *Biochemistry 45*(1), 11-19. doi:10.1021/bi051502y.

Liu, D., & Finley, R. L. (2010). Cyclin Y Is a Novel Conserved Cyclin Essential for Development in *Drosophila*. *Genetics, 184*(4), 1025–1035. http://doi.org/10.1534/genetics.110.114017.

Liu, D., Guest, S., & Finley, R. L. (2010). Why cyclin Y?: A highly conserved cyclin with essential functions. *Fly*, *4*(4), 278–282. http://doi.org/10.4161/fly.4.4.12881.

Lorenzi, H., Khan, A., Behnke, M., et al. (2016). Local admixture of amplified and diversified secreted pathogenesis determinants shapes mosaic *Toxoplasma gondii* genomes. *Nature Communications,*

Lyons, R., McLeod, R. & Roberts, C. (2002) *Toxoplasma gondii* tachyzoite-bradyzoite interconversion. *Trends in Parasitology, 18*(5), 198-201.

Malevich, E., Mirza, A. & Kannan, N. (2011) Structural and evolutionary divergence of eukaryotic protein kinases in Apicomplexa. *BMC Evolutionary Biology*, (11): 321.

Mashayekhi, M., Sandau, M. M., Dunay, I. R., Frickes, E. M., Khan, A., Goldszmid, R. S., Sher, A., Ploegh, H. L., Murphy, T. L., Sibley, L. D. & Murphy, K. M. (2011). $CD8a^{+}$ dendritic cells are the critical source of interleukin-12 that controls acute infection by *Toxoplasma gondii* tachyzoites. *Immunity 35*(2), 249-259.

McAuley, J. B. (2014). Congenital toxoplasmosis. *Journal of the Pediatric Infectious Diseases Society*, (3) Suppl 1, pp. S30–S35, http://doi:10.1093/jpids/piu077.

McFadden, I. & Yeh, E. (2016). The apicoplast: now you see it, now you don't. *International Journal for Parasitology*, *47.* 137-144.

Mikolcevic, P., Rainer, J. & Geley, S. (2012) Orphan kinases turn eccentric: A new class of cyclin Y-activated membrane-targeted CDKs. *Cell Cycle, 11*(20): 3758-3768.

Mikolcevic, P., Sigl, R., Rauch, V., Hess, M. W., Pfaller, K. & Basic, M. (2012). Cyclin-dependent kinase 16/PCTAIRE kinase 1 is activated by cyclin Y and is essential for spermatogenesis. *Mol. Cell Biol, 32*: 868-879.

Moffat, J., Huang, D. & Andrews, B. (2000). Functions of Pho85 cyclin-dependent kinases in budding yeast. *Progress in cell cycle research*, 4: 97-106.

Morgan, D. O. (2007). The cell cycle: Principles of control. Sunderland, MA: Sinauer Associates, Inc. Publishers.

Pappas, G., Roussos, N. & Falagas, M. (2009). Toxoplasmosis snapshots: Global status of *Toxoplasma gondii* seroprevalence and implications for pregnancy and congenital toxoplasmosis. *International Journal for Parasitology, 39* 1385-1394.

Peixoto, L. Chen, F., Harb, O., Davis, P., Beiting, D., Small Brownback, K., Ouloguem, D. & Roos, D. (2010). Integrative genomic approaches highlight a family of parasitic specific kinases that regulate host responses. *Cell Host & Microbe, 8,* 208-218.

Saeij, J. P. J., Boyle, J. P. & Boothroyd, J. C. (2005) Differences among the three major strains of *Toxoplasma gondii* and their specific interactions with the infected host. *Trends in Parasitology*, *21*(10), 476-481. http://doi:10.1016/j.pt.2005.08.001.

Sibley, L. D., Khan, A., Ajioka, J. W. & Rosenthal, B. M. (2009). Genetic diversity of *Toxoplasma gondii* in animals and humans. *Philosophical Transactions of the Royal Society* 364, 2749-2761.

Sidik, S., Huet, D., Ganesan, S., Huynh, M., Wang, T., Nasamu, A., Thiru, P., Saeij, J., Carruthers, V., Niles, J. & Luourido, S. (2016). A genome-wide CRISPR screen in *Toxoplasma* identifies essential Apicomplexan genes. *Cell, 167.* 1-13.

Skariah, S., McIntyre, M. K. & Mordue, D. G. (2010). *Toxoplasma gondii:* determinants of tachyzoite to bradyzoite conversion. *Parasite Res. 2*(107), 253-260.

Stock, A.-K., Dajkic, D., Köhling, H. L., von Heinegg, E. H., Fiedler, M., & Beste, C. (2017). Humans with latent toxoplasmosis display altered reward modulation of cognitive control. *Scientific Reports, 7,* 10170. http://doi.org/10.1038/s41598-017-10926-6.

Sullivan, W. & Jeffers, V. (2011). Mechanisms of *Toxoplasma gondii* persistence and latency. *FEMS Microbiology Reviews*. 717-729.

Torgerson, P. R. & Mastrociacovo, P. (2013). The global burden of congenital toxoplasmosis: a systematic review. Bulletin of the World Health Organization. (91): 7 501-508.

Torrey, E. & Yolken, R. (2013). Toxoplasma oocysts as a public health problem. Trends in Parasitology, (29): 8. 380-384.

Vyas, A., Kim, S. K., Giacomini, N., Boothroyd, J. C. & Sapolsky, R. M. (2007). Behavioral changes induced by Toxoplasma infection of rodents are highly specific to aversion of cat odors. *Proceedings of the National Academy of Science, USA*. 104 (15): 6442-6447. http://doi:10.1073/pnas.0608310104.

Wallace, G. R. & Stanford, M. R. (2008). Immunity and *Toxoplasma* retinochoroiditis. *Clinical and Experimental Immunology* (153), 309-315. http::/doi:10.1111/j. 1365-2249.2008.03692.x

Weiss, L. M. & Dubey, J. P. (2009). Toxoplasmosis: a history of clinical observations. *International Journal of Parasitology, 39*(8), 895-901. http://doi:10.1016/j.ijpara. 2009.02.004.

White, M. W., Radke, J. R. & Radke, J. B. (2014) Toxoplasma development- turn the switch on or off? *Cellular Microbiology 16*(4), 466-472.

Yang, J., Yan, R., Roy, A., Xu, D., Poisson, J. & Zhang, Y. (2012) The I-TASSER Suite: Protein structure and function prediction. *Nature Methods*, *12*, 7-8.